HOKKAIDO UNIVERSITY

Title	On-chip Preparation of Size-controlled PLGA Nanoparticles for Drug Delivery
Author(s)	包, 怡
Degree Grantor	北海道大学
Degree Name	博士(工学)
Dissertation Number	甲第15201号
Issue Date	2022-09-26
DOI	https://doi.org/10.14943/doctoral.k15201
Doc URL	https://hdl.handle.net/2115/87227
Type	doctoral thesis
File Information	BAO_Yi.pdf

Hokkaido University Collection of Scholarly and Academic Papers : HUSCAP

On-chip preparation of size-controlled PLGA nanoparticles for drug delivery

BAO Yi

Graduated School of Chemical Sciences Engineering

Hokkaido University

Doctor Dissertation

Title ON-CHIP PREPARATION OF SIZE-CONTROLLED PLGA NANOPARTICLES FOR DRUG DELIVERY

Author BAO Yi

Supervisor Professor Manabu Tokeshi, Ph.D.

Abstract

Since the introduction of microfluidic devices, they have been widely used in various studies. In recent years, microfluidic devices have been regarded as the most powerful tools for preparing nanoparticles (NPs). By employing microfluidic devices, it is easy and fast to precisely modulate the fluid and thus the properties of the final prepared particles. Nonetheless, the transition from laboratory to clinical applications of poly (lactic-co-glycolic acid) nanoparticles (PLGA NPs) is gradual, partially due to the lack of precision control of each condition in the manufacturing process and the rich selectivity of nanoparticles with varied features. The use of PLGA NPs to create a wide range of size-controlled drug delivery systems and accomplish size-selective drug delivery targeting remains a problem in the development of therapeutics for several illnesses. In this study, a microfluidic device was employed to perform the preparation of PLGA polymer NPs and explored further precision: particle size modulation under the same polymer precursor. The broadened range of applications was achieved: greater particle size selectability for drug-loaded sub-200 nm particles, with greater solvent tolerance. In this context, relevant studies are presented, and the current status of the field is described in Chapter 1.

A microfluidic device was used in Chapter 2 to achieve extensive selectability

for the size of PLGA NPs without alteration of polymer precursors. NPs of specific sizes were created from PLGA, poly (ethylene glycol)-methyl ether block poly (lactic-co-glycolide) (PEG-PLGA), and blended (PLGA + PEG-PLGA). By merely altering the flow rate parameters without modifying the precursor, blended NPs display the largest size range (40–114 nm) (polymer molecular weight, concentration, and chain segment composition). Paclitaxel (PTX), a model hydrophobic drug, was encapsulated in the NPs, and the PTX-loaded NPs had a wide range of adjustable NP sizes. In addition, size-controlled NPs were employed to evaluate the influence of particle size on tumor cell development in sub-200 nm NPs. The 52 nm NPs inhibited cell proliferation more effectively than the 109 nm NPs. This provides a way to achieve further refinement of particle size tailoring by using the desired polymer precursors for preparation. Moreover, this method expands the choice of diverse particle sizes for different needs in the suitable size range (below 200 nm) of NPs for drug delivery.

To improve PLGA NPs usability for drug delivery systems, it is necessary to expand the spectrum of preparation conditions for particle size controllable PLGA NP. This was accomplished utilizing a glass-based microfluidic device and a range of organic solvents in Chapter 3. Four solvents, acetonitrile (ACN), dimethyl sulfoxide (DMSO), dimethylformamide (DMF), and tetrahydrofuran (THF) were employed as solvents to dissolve PLGA and to perform the preparation of NPs, respectively. Additionally, the effect of solvent properties on the particle size and size distribution of the prepared NPs in a non-simple capillary microfluidic device was compared and

discussed. To confirm the ability of glass device to prepare NPs in a large size range, we compared the NPs obtained by the glass device with those prepared by the PDMS device. The glass device was able to maintain a good range of preparable particle sizes of sub-200 nm NPs, although the particle sizes obtained by preparation under the same flow rate conditions were different from those of the PDMS device. To further validate the encapsulation possibilities of different drugs, three distinct kinds of taxanes were used for encapsulation, and PLGA NPs of various sizes (sub-200 nm) were effectively produced. In cellular experiments, the drug-loaded NPs displayed size-dependent cytotoxicity, regardless of the taxane agent utilized. With this chapter, the selectivity is further expanded based on Chapter 2: Solvent Selectivity.

The last chapter concludes this study with the significance of this research in the field. In addition, some future research is proposed based on the current problems that still need to be solved in this study.

Table of Contents

Page

Abstract ..... **ii**

Table of Contents ..... **v**

Abbreviations ..... **viii**

CHAPTER 1 General Introduciton **1**

1.1 Development of PLGA-based DDSs 2

1.1.1 PLGA properties 2

1.1.2 PLGA-based NPs for DDSs 4

1.2 Biodistribution influenced by particle size 8

1.3 PLGA NP preparation methods 11

1.3.1 Particle size-controllable NP preparation by microfluidic devices 14

1.3.2 PDMS microfluidic devices 15

1.4 Present perspective and outline of the thesis 16

References 18

CHAPTER 2 Preparation of size-tunable sub-200 nm PLGA-based nanoparticles with a wide size range using a microfluidic platform **25**

2.1 Introduction 26

2.2 Materials and methods 29

2.2.1 Materials 29

2.2.2 Fabrication of microfluidic devices 30

2.2.3 Preparation of PLGA-based nanoparticles 30

2.2.4 Preparation of PTX-loaded nanoparticles and determination of drug content....31
2.2.5 Cytotoxicity studies....32
2.2.6 Statistical analysis....33
2.3 Results and discussion....33
2.3.1 Effect of the flow conditions on NP size....33
2.3.2 Comparison of the iLiNP device with the conventional method/chaotic mixer device....40
2.3.3 Drug loading into NPs....44
2.3.4 *In vitro* antitumor activity....45
2.4 Conclusion....49
References....51
CHAPTER 3 Effect of organic solvents on the production of PLGA-based drug-loaded nanoparticles using a microfluidic device....56
3.1 Introduction....57
3.2 Experimental....59
3.2.1 Materials....59
3.2.2 Preparation of polymeric NPs....59
3.2.3 Determination of the encapsulation efficiency....60
3.2.4 Cell viability....61
3.2.5 Statistical analysis....61
3.3 Results and discussion....62

3.3.1 Effect of the flow condition on the PLGA NP size 62

3.3.2 Effect of solvent properties on the PLGA NP size 65

3.3.3 Encapsulation of different kinds of anti-cancer drugs 68

3.3.4 Effect of PLGA NP size on cytotoxicity 69

3.4 Conclusions 72

References 74

CHAPTER 4 Conclusion and future prospects 79

4.1 Conclusion 80

4.2 Implications of the research and relationship to previous research 81

4.3 Limitation of this research and future prospect 84

References 86

Acknowledgment 88

Abbreviations

The following abbreviations are used in the manuscript

ACN	acetonitrile
DDS	drug delivery system
DLS	dynamic light scattering
DMAB	didodecyldimethylammonium bromide
DMEM	Dulbecco's modified Eagle's medium
DMF	dimethylformamide;
DMSO	dimethyl sulfoxide;
EE	encapsulation efficiency
FBS	fetal bovine serum
FRR	flow ratio rate
GA	glycolic acid
HPLC	high-performance liquid chromatography;
LA	lactic acid
LNPs	lipid nanoparticles;
Mw	molecular weight
NPs	nanoparticles
PCL	polycaprolactone
PDMS	polydimethylsiloxane
PEA	poly(ethylene adipate)

PEG	polyethylene glycol
PGA	poly(glycolic acid)
PLA	Poly(lactic acid)
PLGA	poly(lactic-co-glycolic-acid)
PTX	paclitaxel
TFR	total flow rate
THF	tetrahydrofuran

CHAPTER 1 General Introduciton

1.1 Development of PLGA-based DDSs

Drug delivery systems (DDSs) are designed to deliver the optimal dose of medication to the body to enhance therapeutic effectiveness and avoid side effects. They are specifically designed to deliver drugs to targeted tissues or organs in a sustainable manner[1,2]. Materials of micron- and nanometer-sized sizes DDSs are used in tissue treatment, engineering, diagnostics, and imaging. Therefore, there has been a lot of study on treatments with enhanced activity and properties. One of the most appealing materials being researched by scientists is polymeric carriers since they can be customized and have their own unique architectures.[3–5].

1.1.1 PLGA properties

In the last few decades, various materials have been used for DDSs, or as biodegradable polymers to aid in drug delivery. Materials that breakdown in vivo by enzymatic, non-enzymatic, or both processes are considered to be biocompatible and toxicologically safe. These by-products are then removed through regular metabolic processes. Biomaterials used to build DDSs can be classified into two broad categories: synthetic biodegradable polymers; and naturally occurring polymers[6]. Typical synthetic biodegradable polymers include poly(lactic acid) (PLA), poly(glycolic acid) (PGA), poly(lactic-co-glycolic acid) (PLGA), polycaprolactone (PCL), poly(ethylene adipate) (PEA) and their copolymers, etc.; and natural polymers include polysaccharides, hyaluronic acid, chitosan, etc.[7,8]. One of the best biodegradable polymers ever generated, PLGA has received US Food and Drug Administration approval for use in medical applications[9][10].

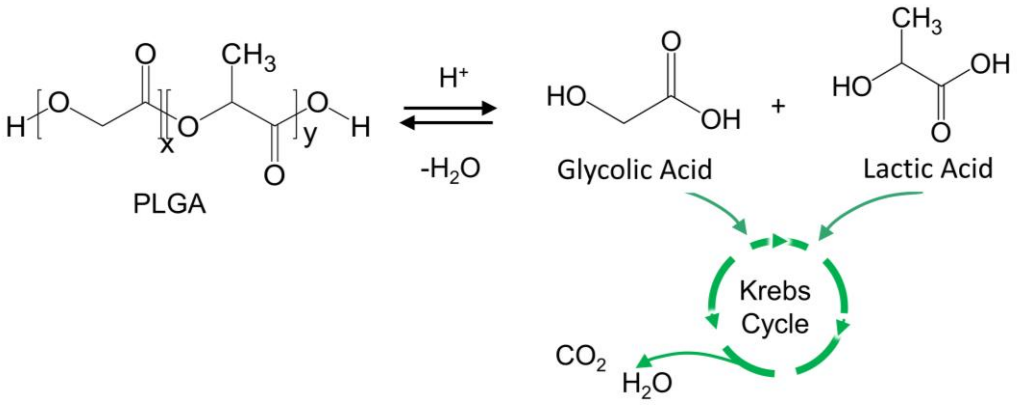

Fig 1.1 Hydrolysis of PLGA (x is the number of lactic acid units and y is the number of glycolic acid units). PLGA is hydrolyzed biologically into lactic and glycolic acids. Endogenous body processes metabolize the hydrolysis products, giving in minimal systemic toxicity.

Understanding the physical, chemical, and biological characteristics of PLGA is crucial for designing more precise drug delivery systems. A copolymer combining PLA and PGA is polyester PLGA. The PGA is a hydrophilic, crystalline polymer that degrades quickly in physiological settings and has a poor water solubility. PLA, in comparison, has a poor mechanical strength and is a stiff hydrophobic polymer[11]. As a copolymer, PLGA has the inherent properties of its constituent monomers. PLGA properties can be tailored to specific applications by simply changing the ratio between LA and GA monomers (Fig 1.1). PLGA contains asymmetric alpha-carbons, which are commonly described in classical stereochemical terminology as the D or L form, and sometimes as the R and S forms, respectively. Poly(D-lactic acid) (PDLA) and poly(L-lactic acid) are the enantiomers of polymeric PLA (PLLA). Poly(D, L-lactic-co-glycolic acid), where the D- and L-lactic forms are present in equal amounts, is known by the abbreviation PLGA. Numerous variables affect the physical and chemical characteristics of PLGA, including molecular weight, PLA to PGA ratio, polymer

concentration, etc.[12–15]. These physical and chemical properties further affect the ability of PLGA to be used as the material for DDSs. Since the polymeric structure prevents drug degradation, the kinetics of drug release from NPs can be controlled via varying the parameters of the formulation (e.g., molecular weight and composition of the polymer, the ratio of polymer to the drug, etc.) to achieve the desired level of sustained drug release.1.1.2 PLGA-based NPs for DDSs

1.1.2 PLGA-based NPs for DDSs

1.1.2.1 Mechanism of cellular internalization

A drug must cross through a sequence of membrane barriers before reaching its site of action in a cell, and at each barrier some amount of the drug is lost. The problems that can potentially overcome by NPs include: cell association and internalization of the drug or drug carriers by endocytosis; intracellular trafficking and cytoplasmic drug release; cytoplasmic translocation of the drug or NPs to the nucleus or other organelles; and nucleus or organelle uptake. A typical intracellular transport route for PLGA-based NPs of a DDS is illustrated in Fig1.2. Overall, the pathway can be broadly divided into seven steps: 1) cell association of NPs; 2) internalization of PLGA NPs into the cell by pinocytosis and by clathrin-mediated endocytosis; 3) endosomal escape of NPs (escape from endo-lysosomes and into the cytoplasm; such an interaction between NPs and the vesicle membrane could result in transient and local instability of the membrane, thus helping NPs escape into the cytosol; 4) drug or therapeutic agent release into the cytoplasm; 5) drug or therapeutic agent transport by cytosol; 6) drug degradation in the

lysosome or cytoplasm; and 7) exocytosis of NPs.

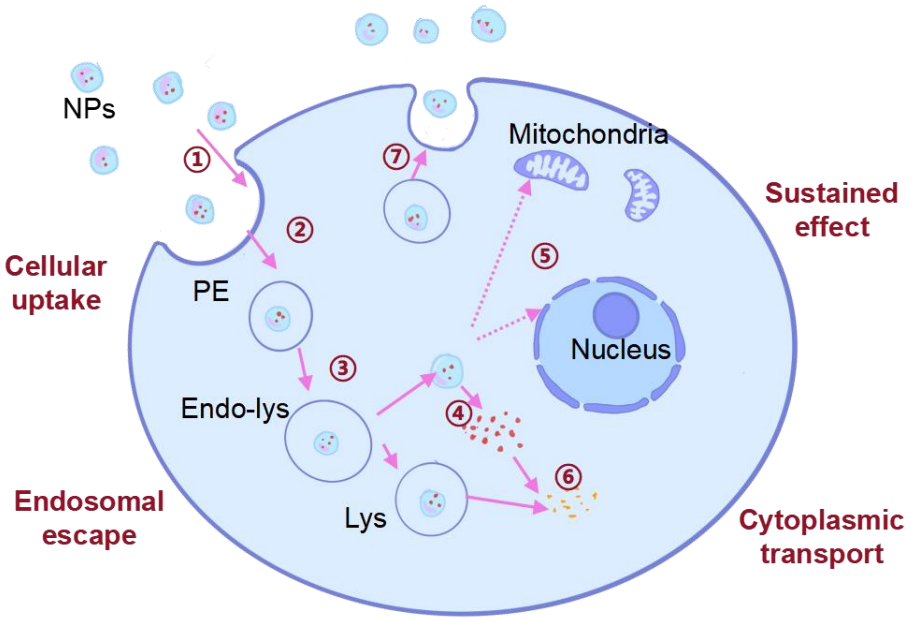

Fig 1.2 Schematic diagram of internalization of PLGA-based NPs of a DDS.[16] The numbers in the squares are the steps as explained in the text. PE, primary endosome; RE, recycling endosome; Endo-lys, endo-lysosome; Lys, lysosome; solid circles, polymeric NPs.

The interaction of drug carriers with the cell membrane and the carriers' endosomal release restricts their efficiency for cytosolic delivery of therapeutic medicines.

1.1.1.2 Challenges to overcome for NP drug delivery - Escape from the reticuloendothelial system

Hydrophobic particles are recognized by the body as foreign. They are removed from the blood circulation system and absorbed into the liver or spleen by the reticuloendothelial system (RES)[17,18]. Conditioner proteins of the serum bond to the

NPs, while other conditioner particles adhere to macrophages and are then absorbed by phagocytosis[19]. This is one of the most significant biological hurdles to overcome for NP-based controlled medication delivery. It can be accomplished by modifying the surface of the NPs to form a hydrophilic layer, resulting in NPs that are not recognized by the RES. To fulfill various drug delivery objectives, a number of PLGA-based block copolymers have been produced, with polyethylene glycol (PEG) being one of the most extensively employed surface-modified segments. When generating NPs from diblock PEG-PLGA, the PEG chains will approach the exterior aqueous phase, functioning as a barrier. Through spatial and hydration repulsions, this barrier can decrease interactions with external molecules, boosting particle stability. It was proved that PEG helped to increase the half-life of PLGA-based NPs in the bloodstream by many orders of magnitude[19]. Other moieties utilized for surface modification include chitosan, and poloxamer, which all prevent the electrostatic and hydrophobic interactions that lead to the binding of conditioners to the surface of NPs. Surface changes enable tumor or organ targeting as well as prevent RES detection. Targeted ligands are commonly attached to the surface of NPs through PEG segments, allowing for selective cell binding and NP ingestion by receptor-mediated endocytosis. When ligands bind NPs, however, caution should be used not just to maintain sufficient affinity for receptor binding, but also to maintain an appropriate PEG coating to avoid RES identification. This necessitates keeping the ligand away from the NP surface in order to prevent being veiled by the PEG chain segments[20–22].

Due to the presence of terminal uncapped terminal carboxylic acid groups of PLGA, PLGA based NPs have a negative surface charge in a neutral pH environment. While the cell membrane is also negatively charged, it is obvious that positively charged particles will establish ionic interactions with the cell membrane more easily compared

to negatively charged particles. By surface modification, PLGA NPs can be transformed into neutral or positively charged particles[23,24].

1.1.1.3 Targeted Cancer Treatment with PLGA-based NPs

The treatment by PLGA-based NPs often involves systemic administration of a drug, which involves off-targeting of the drug resulting in serious side effects. Therefore, targeting strategies have been extensively studied, and they can be broadly classified into two major categories: active targeting and passive targeting.

Active targeting

PLGAs are usually functionalized to achieve targeting. Specific ligands are attached to the surface of the NPs, and the ligands can bind specific receptors or antigens that are overexpressed by tumor cells or tumor vasculature but not by normal cells. The basic principle of this targeting was first proposed by Folkman in 1971: to cause tumor death due to a lack of oxygen and nutrients by destroying the tumor endothelium (as reported in the review by Danhier et al. [23]). Folate receptors, aptamers, antibodies, peptides, and biotin are common ligands for PLGA NPs[20,25–27].

Passive targeting

Passive targeting takes advantage of the size of the NPs and the specific anatomical and pathological abnormalities of a tumor vascular system. The enhanced permeability and retention (EPR) effect was described by Maeda et al.[28]. The tumor's lack of or ineffectual lymphatic capillaries results in the tumor tissue's efficient bottom drainage, which increases retention; additionally, NPs can penetrate and concentrate in the interstitial space, which contributes to increased permeability. Together, these two make up the EPR effect (Fig 1.3). Tumor accumulation by nano ormulations is first based on

the EPR effect, which is considered the gold standard for the design of new anticancer drugs for DDSs. PLGA-based NPs are well suited to utilize passive targeting approaches with the EPR effect due to their properties such as high stability and adjustable extended circulation time[29–32].

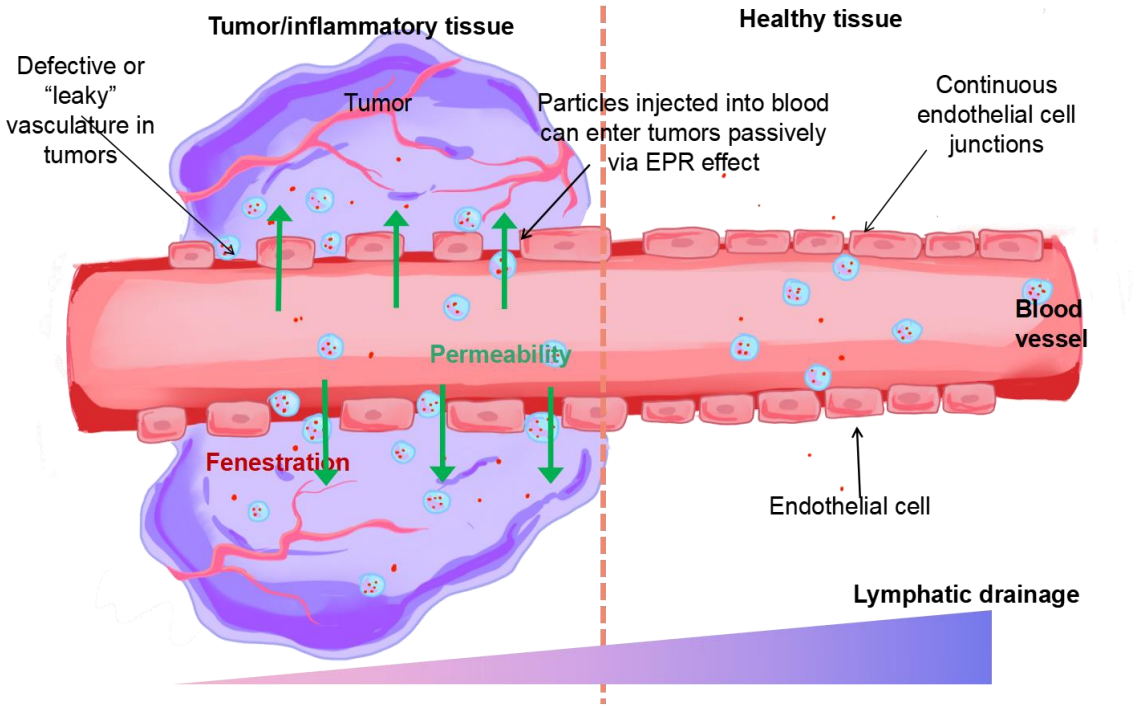

Fig 1.3 Escape of NPs into healthy tissue or tumor-associated vessels.

However, there are some problems with passive targeting alone: the EPR effect may vary with the patient, tumor type, and time[33–37]. This inter- and intra-tumor variability has lead researchers to consider that an important topic for the clinical applications of NPs is individualized and tailored anticancer nanomedicine therapy.

1.2 Biodistribution influenced by particle size

Among the modes of administration, intravenous administration is one of the most commonly used approaches. NPs administered intravenously circulate throughout the body. The NPs escape from the circulatory system to other tissues by endocytosis,

shear-induced diffusion, or passive diffusion through open windows in the capillary network. Particles larger than 200 nm will be trapped in the spleen, so ideally, long-circulating NPs are not hardened beyond 200 nm to avoid clearance[38,39]. Meanwhile, the EPR effect mentioned in section 1.1.2.3 is usually limited to NPs between 30-200 nm, which can escape the circulatory system through openings within the capillary network of tumor tissue[40,41]. Fig 1.4 collates the size factors that need to be considered for designing NPs for DDSs. In addition, tumor heterogeneity results in a cutoff size that can vary between tumors and even within the same tumor. The vascular system will exhibit different porosities and thus different infiltration rates[42,43].

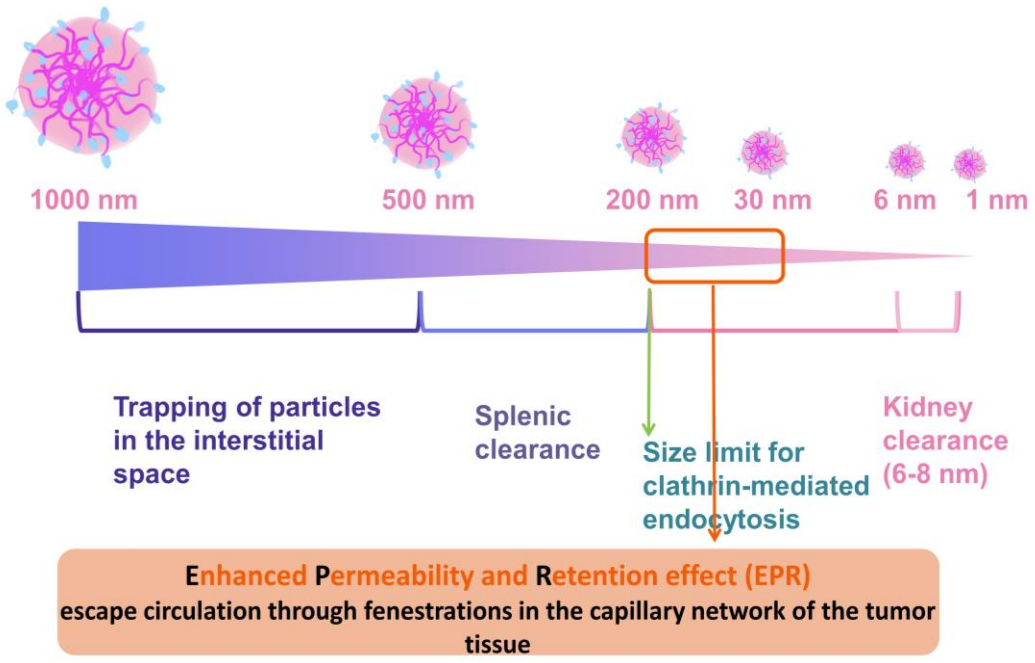

Fig 1.4 Particle size is an important variable to consider when designing NPs for DDSs.

The effect of particle size on the *in vivo* distribution has been reported by several studies. Results Wang et al.[44] compared the particle size dependence of 70, 110, and 150 nm NPs in HepG2 and H22 cells. Their results showed that the 110 nm tumor/liver ratio was the largest of the three particle sizes. Cabral et al. [45] compared the different

accumulations of 30, 50, 70, and 100 nm polymeric particles in tumors in detail. In high permeability BXPCx tumors, they found no particle size effect was shown. However, in low permeability C26 tumors, 30 nm particles showed a greater therapeutic advantage, followed by 50 nm NPs. Choi et al. [46] compared the cellular uptake of PLGA-based NPs in KB cells, and the size dependence was more prominent between 70-200 nm, while it was relatively insignificant between 400-1000 nm. Among them, 70 nm NPs showed the highest cellular uptake. Win et al.[47] reported on the particle size effect of PLGA NPs in Caco-2 at 50, 100, 200, 500, and 1000 nm NPs. The 100 nm particles showed higher cellular uptake than 50 nm particles and were the most taken up particles. The report of Xu et al. [48] confirmed the earlier findings of Win et al. Xu et al. compared the difference in cellular uptake at 50 nm, 100 nm, 150 nm, 200 nm, and 300 nm in Caco-2 and HT-29 cells. Instead of smaller NPs showing higher cellular uptake, the 100 nm NPs showed higher cellular uptake. In 2010, Saez et al. [49] reported on the difference in biodistribution of 100 nm vs. 160 nm polymeric NPs in different tissues. The latter NPs had higher liver aggregation compared to the kidney and spleen. In contrast, 110 nm particles had essentially the same distribution in the liver-kidney, and spleen. Zhang et al. [50] investigated the biodistribution of NPs at 80,107 and 180 nm. Particles of the same size showed different biodistributions in the kidney, liver, lung, and spleen. In addition, at the same sampling time, the 80 nm particles showed a higher biodistribution than the 107 nm and 180 nm NPs in the blood.

These results suggest that the "particle size optimal solution" for therapeutic NPs is different for different cells or tissues. Since pathophysiology is extremely complex, there is a need to provide a stable preparation method that can precisely modulate the particle size of sub-200 nm PLGA-based NPs to support drug screening and to support

studying of particle size effects.

1.3 PLGA NP preparation methods

The technology for producing NPs plays an important role in their final characteristics such as shape, size, size distribution, and stability. A wide range of techniques has been used for the synthesis of PLGA-based NPs. The preparation methods can be broadly classified as top-down and bottom-up[51][9] (Fig 1.5). In the top-down approaches, physical methods are used to convert particles to the nanoscale. On the one hand, these methods are easy to scale-up for industrial use, and they provide a fine-particle production capacity, but on the other hand they are costly and energy-intensive in terms of equipment and they are not conducive to rapid drug screening.Spray drying is one of the most commonly used techniques for producing NPs. Spray drying process need to be realized by an atomizer and a hot dry air stream. The liquid feed consists of polymer and drug particles, which are dispersed into fine droplets by the atomizer. The spray drying method has simple steps that can be scaled up and it does not require particle separation. Despite its many advantages, spray drying is not applicable to heat-sensitive materials. The NPs produced tend to agglomerate during processing, resulting in submicron to micron-sized particles, which leads to reduced particle size control. In addition, there are difficulties such as low product yields and sticking. Usually, the low yield is due to product loss on the drying chamber walls, which is also responsible for high maintenance costs. All these factors lead to the inappropriateness of the spray drying technique to produce NPs for rapid drug screening by DDSs at laboratory scale.

Bottom-up approaches are based on the self-assembly properties of macromolecules. Polymers, due to their amphiphilic nature, self-assemble into particles

during the mixing of polymeric organic solvents with non-solvents. Commonly used bottom-up methods include emulsification-evaporation and nanoprecipitation methods. The former involves dissolving the polymer in an organic solvent that is not miscible with water. The organic solution is added to the aqueous phase containing the surfactant under continuous stirring. This is followed by evaporation to achieve an oil/water (O/W) (or the reverse W/O) form. Further, it is possible to change from a single emulsion method to a double emulsion method, i.e., the primary oil-in-water emulsion is added to a second oil phase containing a stabilizer, resulting in an O/W/O (or the reverse W/O/W) emulsion.

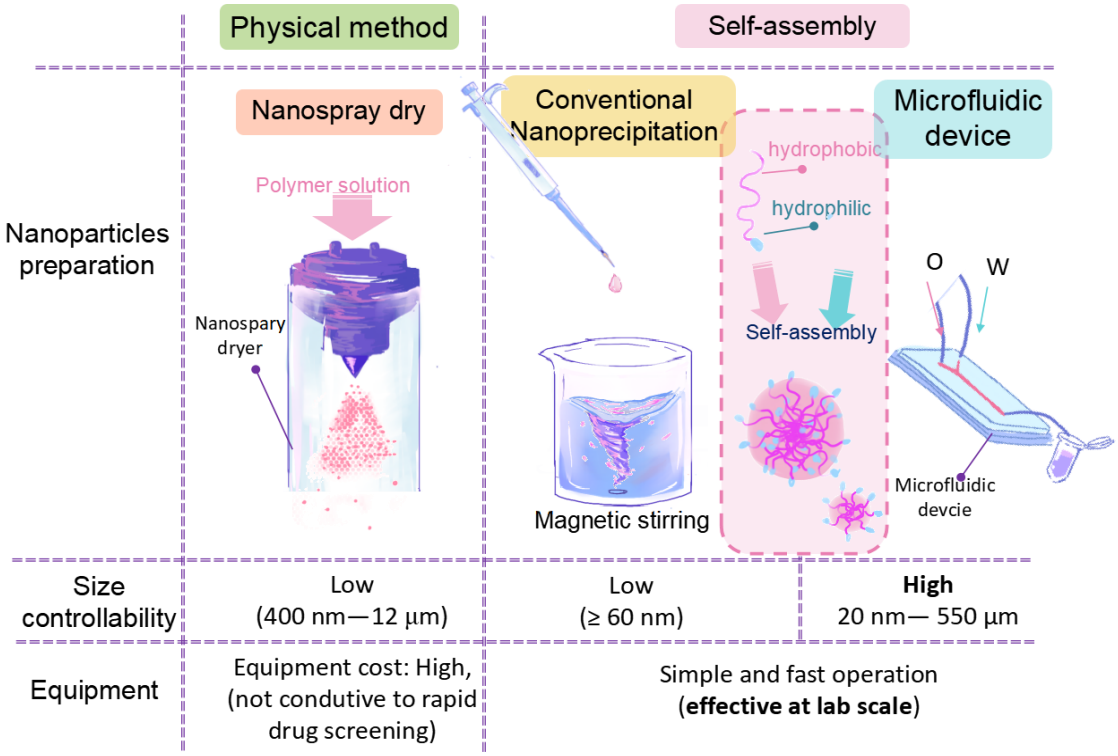

Fig 1.5 PLGA NP preparation method

Nanoprecipitation, also called solvent displacement, is a one-step method. The polymer and drug are dissolved in an organic solvent that is miscible with water, and then a liquid drop is added to the aqueous phase. At the same time, rapid solvent diffusion, and particles are formed.

The self-assembly-based method is simple and fast, and the required stirring device is less energy-intensive and more efficient on an experimental scale. However, the method has some drawbacks, such as significant batch-to-batch variation and uncontrolled particle growth. In addition, since the speed of adding the organic solution to the aqueous phase also affects the final particle formation, many times researchers have chosen to use a pipette gun to add solution drop-by-drop rather than pouring directly. This leads to labor-intensive operations and the entire process is not sufficiently microscale for fluid control to achieve the desired accuracy of particle size design and regulation.

Microfluidic methods represent a new approach and they have received a lot of attention in recent years. A microfluidic device is a device that realizes a reaction in a channel with an inner diameter of less than 1 mm. A simple microreactor system includes a pump to control the syringe, inlet tubes linking the syringe and the microfluidic device, outlet tubes from the device, and a container to collect the product. The syringe pump settings are adjusted for simple operation and non-labor-intensive fluid manipulation. The small channel size of the microfluidic device offers the possibility of handling or manipulating microliters or even nanoliters of fluid. In contrast to conventional methods, microfluidic devices can precisely control the mixing of fluids by controlling the fluid conditions, which greatly affect the process of NP formation and should ultimately affect the various properties of the particles formed. In summary, preparing NPs by microfluidic devices requires very little fluid and is non-labor intensive, with a controlled mixing process, making it well suited for rapid screening of drugs[51,52].

1.3.1 Particle size-controllable NP preparation by microfluidic devices

Microfluidic devices have become the ideal choice for NP preparation because of their tunability for NPs (size, shape, surface properties, etc.), good reproducibility between batches, and other characteristics.

As described in section 1.2, particle size is one of the most important properties of PLGA NPs. And to provide better particle size selectivity, most microfluidic devices resort to changing polymer precursors, such as the molecular weight of the polymer, polymer composition, solution concentration, etc. Karnik et al. [53] employed a flow-focusing microfluidic device to produce NPs in the 30–105 nm range by adding PLGA to poly(ethylene glycol) methyl ether-block-poly(lactic-co-glycolide) (PEG-PLGA) in various proportions. Valencia et al. [54] exploited Tesla structures in a microchannel and they made NPs with an average particle size of 35–180 nm by varying the PLGA and DSPE-PEG composition and concentration. Rhee et al. [55] synthesized NPs with a particle size of 30–230 nm by altering the molecular weight and PLGA concentration. The study by Valencia et al. [56] reported the use of a 3D hydrodynamically focused device to prepare NPs. Different ratios of PLGA to PEG-PLGA mix composition ratios, or changes in the chain segment length of PEG-PLGA were used to obtain particles of 25-200 nm in size.

These polymer precursors (molecular weight, composition orthe solution concentration) need to be altered in manually formulated solutions prior to injection into the microfluidic devices, and if these conditions must be altered, it means that the advantage of less labor-intensive is lost. In addition, the precursors of the macromolecules greatly influence other properties of the NPs, such as biodistributability. Therefore, if it is not possible to achieve a wide range of

controllability of particle size without changing the polymer precursors, then it is not possible to meet the high precision needs of particle size impact studies and future clinical customization needs.

1.3.2 PDMS microfluidic devices

Polydimethylsiloxane (PDMS) is the most commonly used material for making microfluidic devices. PDMS is inexpensive and has good permeability and optical properties. It is also easily molded to form the devices and can accommodate a variety of different complex geometries, providing great flexibility for geometric control[57–59]. Fig 1.6 shows the whole process of PDMS device fabrication from preparing the mold to preparing the PDMS-glass device.

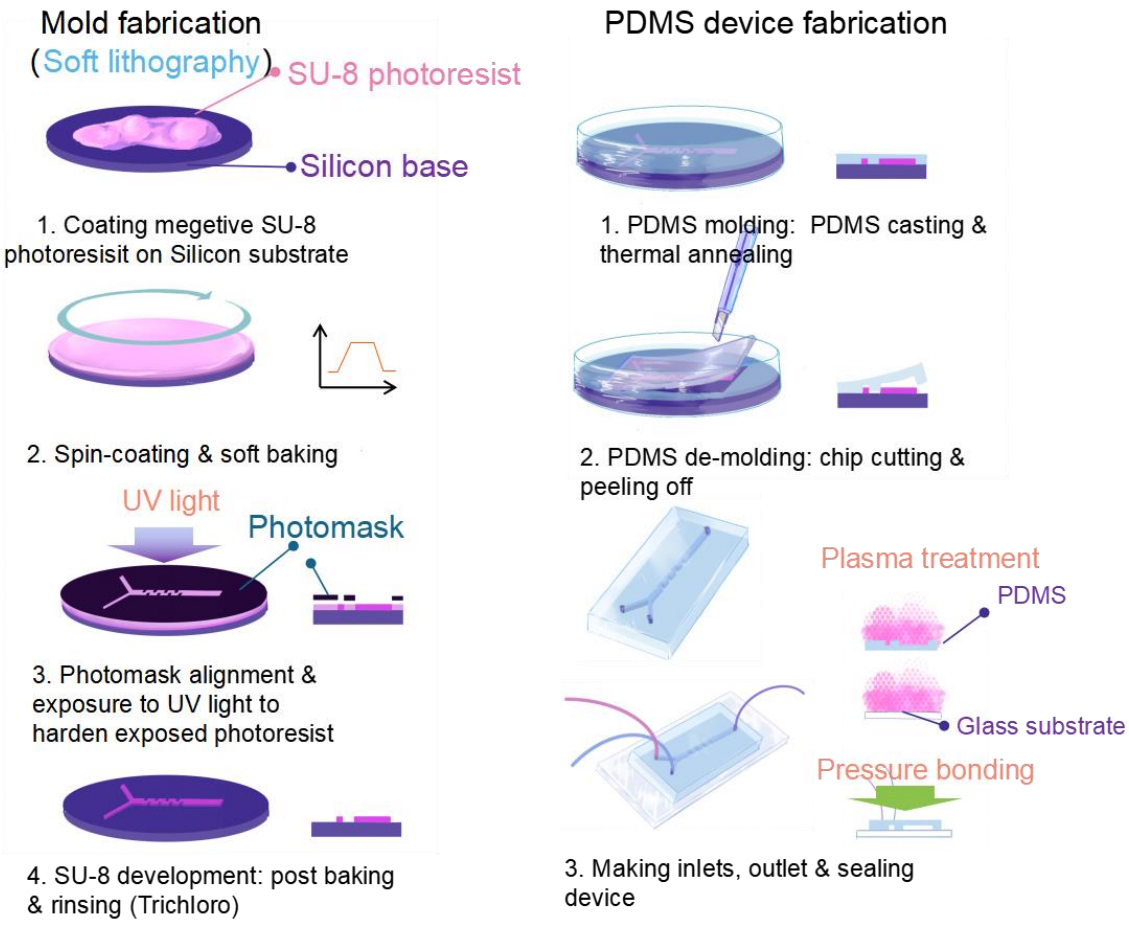

Fig 1.6 PDMS device fabrication.

PDMS has some compatibility issues with certain solvents, and it swells or even peels off the glass substrate when contacting with some organic solvents. This places a big limitation on the solvents that can be used in the PDMS device fabrication[57,60].

1.4 Present perspective and outline of the thesis

As described in section 1.3, microfluidic devices can be effectively utilized to produce NPs; however, most methods to achieve good particle selectivity involve altering the precursors of the macromolecules. In turn, changing the precursors means that different solutions need to be manually and repeatedly formulated before injection into the microfluidic devices. If 1tion, the precursors of the macromolecules greatly influence other properties of the particles, such as biodistributability. Therefore, if it is not possible to achieve a wide range of controllability of particle size without changing the polymer precursors; then, it is not possible to meet the high precision needs of particle size impact studies and to further clinical customization needs. Consequently, there is an urgent need to provide a method to achieve the simple and convenient preparation of PLGA-based NPs without changing polymer precursors. This method should make it possible for researchers to achieve a greater range of NP size selectivity.

In addition, while PDMS devices offer a wide variety of design options, they are limited by solvent compatibility issues. However, during drug screening, the solubility of different drugs in organic solvents varies, and in addition, by changing the solvent, the precipitation time of the drug can also be changed so that the drug precipitation time can be adjusted to be as close as possible to that of the macromolecules. Achieving similar precipitation times can be expected to allow the polymer NPs to encapsulate the drug better[61]. This means that it is also necessary to provide different solvents selectively.

To address these limitations, this thesis study has been conducted as follows.

In chapter 2, a microfluidic device was used to obtain unaltered polymeric precursors to achieve a wide range of particle size modulations, thus further improving precision and expanding the selectivity for size and polymer precursor customed NP preparation. In chapter 3, a glass microfluidic device was used to investigate broadening the range of suitable solvents in applications of solvent screening and drug screening with guaranteed particle size controllability. Finally, in chapter 4, the conclusions, implications and future perspectives were discussed.

References

1. Mu W, Chu Q, Liu Y, Zhang N. A Review on Nano-Based Drug Delivery System for Cancer Chemoimmunotherapy. Nano-Micro Letters 2020 12:1. 2020;12: 1–24. doi:10.1007/S40820-020-00482-6
2. Kingsley JD, Dou H, Morehead J, Rabinow B, Gendelman HE, Destache CJ. Nanotechnology: A Focus on Nanoparticles as a Drug Delivery System. Journal of Neuroimmune Pharmacology 2006 1:3. 2006;1: 340–350. doi:10.1007/S11481-006-9032-4
3. Sur S, Rathore A, Dave V, Reddy KR, Chouhan RS, Sadhu V. Recent developments in functionalized polymer nanoparticles for efficient drug delivery system. Nano-Structures & Nano-Objects. 2019;20: 100397. doi:10.1016/J.NANOSO.2019.100397
4. Lepeltier E, Bourgaux C, Couvreur P. Nanoprecipitation and the “Ouzo effect”: Application to drug delivery devices. Advanced Drug Delivery Reviews. Elsevier; 2014. pp. 86–97. doi:10.1016/j.addr.2013.12.009
5. Masserini M. Nanoparticles for Brain Drug Delivery. ISRN Biochemistry. 2013;2013: 238428. doi:10.1155/2013/238428
6. Hirenkumar M, Steven S. Poly Lactic-co-Glycolic Acid (PLGA) as Biodegradable Controlled Drug Delivery Carrier. Polymers. 2012;3: 1–19. doi:10.3390/polym3031377.Poly
7. Anderson JM, Shive MS. Biodegradation and biocompatibility of PLA and PLGA microspheres. Advanced Drug Delivery Reviews. 1997;28: 5–24. doi:10.1016/S0169-409X(97)00048-3
8. Uhrich KE, Cannizzaro SM, Langer RS, Shakesheff KM. Polymeric Systems for Controlled Drug Release. Chemical Reviews. 1999;99: 3181–3198. doi:10.1021/CR940351U
9. Rezvantalab S, Keshavarz Moraveji M. Microfluidic assisted synthesis of PLGA drug delivery systems. RSC Advances. Royal Society of Chemistry; 2019. pp. 2055–2072. doi:10.1039/C8RA08972H
10. Danhier F, Lecouturier N, Vroman B, Jérôme C, Marchand-Brynaert J, Feron O, et al. Paclitaxel-loaded PEGylated PLGA-based nanoparticles: In vitro and in vivo evaluation. Journal of Controlled Release. 2009;133: 11–17.

doi:10.1016/J.JCONREL.2008.09.086

11. Makadia HK, Siegel SJ. Poly Lactic-co-Glycolic Acid (PLGA) as Carrier. Polymers. 2011;3: 1377–1397. doi:10.3390/polym3031377
12. Houchin ML, Topp EM. Physical properties of PLGA films during polymer degradation. Journal of Applied Polymer Science. 2009;114: 2848–2854. doi:10.1002/APP.30813
13. Passerini N, Craig DQM. An investigation into the effects of residual water on the glass transition temperature of polylactide microspheres using modulated temperature DSC. Journal of Controlled Release. 2001;73: 111–115. doi:10.1016/S0168-3659(01)00245-0
14. Siegel SJ, Kahn JB, Metzger K, Winey KI, Werner K, Dan N. Effect of drug type on the degradation rate of PLGA matrices. European Journal of Pharmaceutics and Biopharmaceutics. 2006;64: 287–293. doi:10.1016/J.EJPB.2006.06.009
15. Yang YY, Chung TS, Ping Ng N. Morphology, drug distribution, and in vitro release profiles of biodegradable polymeric microspheres containing protein fabricated by double-emulsion solvent extraction/evaporation method. Biomaterials. 2001;22: 231–241. doi:10.1016/S0142-9612(00)00178-2
16. Vasir JK, Labhasetwar V. Biodegradable nanoparticles for cytosolic delivery of therapeutics. Advanced Drug Delivery Reviews. 2007;59: 718–728. doi:10.1016/J.ADDR.2007.06.003
17. Danhier F, Ansorena E, Silva JM, Coco R, Le Breton A, Préat V. PLGA-based nanoparticles: An overview of biomedical applications. Journal of Controlled Release. 2012;161: 505–522. doi:10.1016/J.JCONREL.2012.01.043
18. Kumari A, Yadav SK, Yadav SC. Biodegradable polymeric nanoparticles based drug delivery systems. Colloids and Surfaces B: Biointerfaces. 2010;75: 1–18. doi:10.1016/J.COLSURFB.2009.09.001
19. Bortolussi R, Mailman TL. Listeriosis. Infectious Diseases of the Fetus and Newborn Infant. 2010; 470–488. doi:10.1016/B978-1-4160-6400-8.00013-4
20. Kocbek P, Obermajer N, Cegnar M, Kos J, Kristl J. Targeting cancer cells using PLGA nanoparticles surface modified with monoclonal antibody. Journal of Controlled Release. 2007;120: 18–26. doi:10.1016/J.JCONREL.2007.03.012
21. Croll TI, O'Connor AJ, Stevens GW, Cooper-White JJ. Controllable surface modification of poly(lactic-co-glycolic acid) (PLGA) by hydrolysis or aminolysis I: Physical, chemical, and theoretical aspects. Biomacromolecules.

2004;5: 463–473. doi:10.1021/BM0343040/ASSET/IMAGES/LARGE/BM0343040F00010.JPEG

22. Müller M, Vörös J, Csúcs G, Walter E, Danuser G, Merkle HP, et al. Surface modification of PLGA microspheres. Journal of Biomedical Materials Research Part A. 2003;66A: 55–61. doi:10.1002/JBM.A.10502
23. Danhier F, Feron O, Préat V. To exploit the tumor microenvironment: Passive and active tumor targeting of nanocarriers for anti-cancer drug delivery. Journal of Controlled Release. 1971;285: 1182–1186. doi:10.1016/J.JCONREL.2010.08.027
24. Wang M, Thanou M. Targeting nanoparticles to cancer. Pharmacological Research. 2010;62: 90–99. doi:10.1016/J.PHRS.2010.03.005
25. Stroock AD, Dertinger SKW, Ajdari A, Mezić I, Stone HA, Whitesides GM. Chaotic mixer for microchannels. Science. 2002;295: 647–651. doi:10.1126/science.1066238
26. Martins C, Sousa F, Araújo F, Sarmento B. Functionalizing PLGA and PLGA Derivatives for Drug Delivery and Tissue Regeneration Applications. Advanced Healthcare Materials. 2018;7: 1701035. doi:10.1002/ADHM.201701035
27. Esmaeili F, Ghahremani MH, Ostad SN, Atyabi F, Seyedabadi M, Malekshahi MR, et al. Folate-receptor-targeted delivery of docetaxel nanoparticles prepared by PLGA–PEG–folate conjugate. http://dx.doi.org/101080/10611860802088630. 2008;16: 415–423. doi:10.1080/10611860802088630
28. Maeda H, Wu J, Sawa T, Matsumura Y, Hori K. Tumor vascular permeability and the EPR effect in macromolecular therapeutics: a review. Journal of Controlled Release. 2000;65: 271–284. doi:10.1016/S0168-3659(99)00248-5
29. Narayanan S, Mony U, Vijaykumar DK, Koyakutty M, Paul-Prasanth B, Menon D. Sequential release of epigallocatechin gallate and paclitaxel from PLGA-casein core/shell nanoparticles sensitizes drug-resistant breast cancer cells. Nanomedicine: Nanotechnology, Biology and Medicine. 2015;11: 1399–1406. doi:10.1016/J.NANO.2015.03.015
30. Ramazani F, Chen W, Van Nostrum CF, Storm G, Kiessling F, Lammers T, et al. Strategies for encapsulation of small hydrophilic and amphiphilic drugs in PLGA microspheres: State-of-the-art and challenges. International Journal of Pharmaceutics. 2016;499: 358–367. doi:10.1016/J.IJPHARM.2016.01.020

31. Moreno D, Zalba S, Navarro I, Tros de Ilarduya C, Garrido MJ. Pharmacodynamics of cisplatin-loaded PLGA nanoparticles administered to tumor-bearing mice. European Journal of Pharmaceutics and Biopharmaceutics. 2010;74: 265–274. doi:10.1016/J.EJPB.2009.10.005
32. Park JS, Qiao L, Su ZZ, Hinman D, Willoughby K, McKinstry R, et al. Ionizing radiation modulates vascular endothelial growth factor (VEGF) expression through multiple mitogen activated protein kinase dependent pathways. Oncogene 2001 20:25. 2001;20: 3266–3280. doi:10.1038/sj.onc.1204258
33. Danhier F. To exploit the tumor microenvironment: Since the EPR effect fails in the clinic, what is the future of nanomedicine? Journal of Controlled Release. 2016;244: 108–121. doi:10.1016/J.JCONREL.2016.11.015
34. Lammers T, Kiessling F, Hennink WE, Storm G. Drug targeting to tumors: Principles, pitfalls and (pre-) clinical progress. Journal of Controlled Release. 2012;161: 175–187. doi:10.1016/J.JCONREL.2011.09.063
35. Theek B, Gremse F, Kunjachan S, Fokong S, Pola R, Pechar M, et al. Characterizing EPR-mediated passive drug targeting using contrast-enhanced functional ultrasound imaging. Journal of Controlled Release. 2014;182: 83–89. doi:10.1016/J.JCONREL.2014.03.007
36. Dasgupta A, Liu M, Ojha T, Storm G, Kiessling F, Lammers T. Ultrasound-mediated drug delivery to the brain: principles, progress and prospects. Drug Discovery Today: Technologies. 2016;20: 41–48. doi:10.1016/J.DDTEC.2016.07.007
37. Shi Y, Zhou M, Zhang J, Lu W. Preparation and cellular targeting study of VEGF-conjugated PLGA nanoparticles. https://doi.org/103109/0265204820151035683. 2015;32: 699–704. doi:10.3109/02652048.2015.1035683
38. Scott SM, Ali Z. Fabrication Methods for Microfluidic Devices: An Overview. Micromachines 2021, Vol 12, Page 319. 2021;12: 319. doi:10.3390/MI12030319
39. Allen S, Liu YG, Scott E. Engineering Nanomaterials to Address Cell-Mediated Inflammation in Atherosclerosis. Regenerative Engineering and Translational Medicine 2016 2:1. 2016;2: 37–50. doi:10.1007/S40883-016-0012-9
40. Jhaveri AM, Torchilin VP. Multifunctional polymeric micelles for delivery of drugs and siRNA. Frontiers in Pharmacology. 2014;5 APR: 77. doi:10.3389/FPHAR.2014.00077/BIBTEX

41. Jain RK, Stylianopoulos T. Delivering nanomedicine to solid tumors. Nature Reviews Clinical Oncology 2010 7:11. 2010;7: 653–664. doi:10.1038/nrclinonc.2010.139
42. Augmentation of Transvascular Transport of Macromolecules and Nanoparticles in Tumors Using Vascular Endothelial Growth Factor1 | Cancer Research | American Association for Cancer Research. [cited 18 Jun 2022]. Available: https://aacrjournals.org/cancerres/article/59/16/4129/505388/Augmentation-of-Transvascular-Transport-of
43. Prabhakar U, Maeda H, K. Jain R, Sevick-Muraca EM, Zamboni W, Farokhzad OC, et al. Challenges and key considerations of the enhanced permeability and retention effect for nanomedicine drug delivery in oncology. Cancer Research. 2013;73: 2412–2417. doi:10.1158/0008-5472.CAN-12-4561/651197/AM/CHALLENGES-AND-KEY-CONSIDERATIONS-OF-THE-ENHANCED
44. Wang J, Wu W, Zhang Y, Wang X, Qian H, Liu B, et al. The combined effects of size and surface chemistry on the accumulation of boronic acid-rich protein nanoparticles in tumors. Biomaterials. 2014;35: 866–878. doi:10.1016/J.BIOMATERIALS.2013.10.028
45. Cabral H, Matsumoto Y, Mizuno K, Chen Q, Murakami M, Kimura M, et al. Accumulation of sub-100 nm polymeric micelles in poorly permeable tumours depends on size. Nature Nanotechnology. 2011;6: 815–823. doi:10.1038/nnano.2011.166
46. Choi JS, Cao J, Naeem M, Noh J, Hasan N, Choi HK, et al. Size-controlled biodegradable nanoparticles: Preparation and size-dependent cellular uptake and tumor cell growth inhibition. Colloids and Surfaces B: Biointerfaces. 2014;122: 545–551. doi:10.1016/J.COLSURFB.2014.07.030
47. Win KY, Feng S-S. Effects of particle size and surface coating on cellular uptake of polymeric nanoparticles for oral delivery of anticancer drugs. Biomaterials. 2005;26: 2713–2722. doi:10.1016/j.biomaterials.2004.07.050
48. Xu A, Yao M, Xu G, Ying J, Ma W, Li B, et al. A physical model for the size-dependent cellular uptake of nanoparticles modified with cationic surfactants. International Journal of Nanomedicine. 2012;7: 3547–3554. doi:10.2147/IJN.S32188
49. Saez A, Guzmán M, Molpeceres J, Aberturas MR. Freeze-drying of polycaprolactone and poly(d,l-lactic-glycolic) nanoparticles induce minor

particle size changes affecting the oral pharmacokinetics of loaded drugs. European Journal of Pharmaceutics and Biopharmaceutics. 2000;50: 379–387. doi:10.1016/S0939-6411(00)00125-9

50. Zhang L, Hu Y, Jiang X, Yang C, Lu W, Yang YH. Camptothecin derivative-loaded poly(caprolactone-co-lactide)-b-PEG-b- poly(caprolactone-co-lactide) nanoparticles and their biodistribution in mice. Journal of Controlled Release. 2004;96: 135–148. doi:10.1016/j.jconrel.2004.01.010
51. Shrimal P, Jadeja G, Patel S. A review on novel methodologies for drug nanoparticle preparation: Microfluidic approach. Chemical Engineering Research and Design. 2020;153: 728–756. doi:10.1016/J.CHERD.2019.11.031
52. Liu Y, Yang G, Hui Y, Ranaweera S, Zhao C-X, Liu Y, et al. Microfluidic Nanoparticles for Drug Delivery. Small. 2022; 2106580. doi:10.1002/SMLL.202106580
53. Karnik R, Gu F, Basto P, Cannizzaro C, Dean L, Kyei-Manu W, et al. Microfluidic Platform for Controlled Synthesis of Polymeric Nanoparticles. Nano Letters. 2008;8: 2906–2912. doi:10.1021/nl801736q
54. Valencia PM, Basto PA, Zhang L, Rhee M, Langer R, Farokhzad OC, et al. Single-Step Assembly of Homogenous Lipid−Polymeric and Lipid−Quantum Dot Nanoparticles Enabled by Microfluidic Rapid Mixing. ACS Nano. 2010;4: 1671–1679. doi:10.1021/nn901433u
55. Rhee M, Valencia PM, Rodriguez MI, Langer R, Farokhzad OC, Karnik R. Synthesis of Size-Tunable Polymeric Nanoparticles Enabled by 3D Hydrodynamic Flow Focusing in Single-Layer Microchannels. Advanced Materials. 2011;23: H79–H83. doi:10.1002/adma.201004333
56. Valencia PM, Pridgen EM, Rhee M, Langer R, Farokhzad OC, Karnik R. Microfluidic Platform for Combinatorial Synthesis and Optimization of Targeted Nanoparticles for Cancer Therapy. ACS Nano. 2013;7: 10671–10680. doi:10.1021/nn403370e
57. Choi WM, Park OO. A soft-imprint technique for direct fabrication of submicron scale patterns using a surface-modified PDMS mold. Microelectronic Engineering. 2003;70: 131–136. doi:10.1016/S0167-9317(03)00436-2
58. Whitesides GM. The origins and the future of microfluidics. Nature 2006 442:7101. 2006;442: 368–373. doi:10.1038/nature05058
59. Shih TK, Chen CF, Ho JR, Chuang FT. Fabrication of PDMS

(polydimethylsiloxane) microlens and diffuser using replica molding. Microelectronic Engineering. 2006;83: 2499–2503. doi:10.1016/J.MEE.2006.05.006

60. Roman GT, Culbertson CT. Surface engineering of poly(dimethylsiloxane) microfluidic devices using transition metal sol-gel chemistry. Langmuir. 2006;22: 4445–4451. doi:10.1021/LA053085W/ASSET/IMAGES/LARGE/LA053085WF00008.JPEG

61. Li W, Chen Q, Baby T, Jin S, Liu Y, Yang G, et al. Insight into drug encapsulation in polymeric nanoparticles using microfluidic nanoprecipitation. Chemical Engineering Science. 2021;235: 116468. doi:10.1016/J.CES.2021.116468

CHAPTER 2 Preparation of size-tunable sub-200 nm PLGA-based nanoparticles with a wide size range using a microfluidic platform

2.1 Introduction

Over the past decades, polymeric nanoparticles (NPs), especially biodegradable polymers, have emerged for building a drug delivery system (DDS)[1–3]. NPs comprising poly(lactic-co-glycolic-acid) (PLGA) have been widely used as carriers for hydrophilic and hydrophobic drugs, as well as proteins, vaccines, and siRNA[4–7], owing to their excellent biodegradability and biocompatibility[8]. By employing PLGA, countless laboratory synthesis methods present novel PLGA-based NPs targeting and inhibiting cancer cells; nevertheless, only a minority of formulations have achieved clinical translation and effects on humans[9–12]. To some extent, the challenge lies with the complexity of NP optimization. For every disease type, it is essential to find the optimal physicochemical parameters (such as particle size, surface charge, morphology, and rigidity) and assess tissue targeting, designed drug release, and immune evasion.

In KB carcinoma cell lines, 70 nm-sized PLGA NPs took up more than 200 nm-sized PLGA NPs, whereas, in RAW264.7 macrophages, 70 nm-sized NP engulfment was less than 200 nm-sized NPs[13]. In two human colon cancer cell lines (Caco-2 and HT-29 cells), the cellular uptake rate of 100 nm-sized didodecyldimethylammonium bromide (DMAB)-modified PLGA NPs was higher than that of 50 nm-sized NPs[14]. The uptake of 100 nm particles in Caco-2 cell lines was 2.3 times greater than that of 50 nm-sized NPs[15]. These results indicate that NPs sized approximately 100 nm have a profound size effect (from 50 nm to 200 nm). Precise preparation of particle-size-controlled NPs is of great significance for establishing different targeted drug delivery systems. Particle size is a crucial feature in the DDS design, which determines the in *vivo* distribution, cytotoxicity, and stability of NPs and influences drug loading and release[16]. The particle size can control the particle distribution in the body to some

extent[4,17,18]. Therefore, preparing polymeric NPs with a controllable size is critical to precisely control drug loading and release and, more importantly, realizing building size-targeted DDS. To extensively investigate various disease types, a wide range of size-controlled PLGA-based NPs at the nanoscale level is imperative. Generally, to approach size controlled PLGA NPs with a broad size range, researchers tend to change the polymer precursors (polymer composition, concentration, and molecular weight (Mw)). However, changes in precursor condition would interfere with NP characteristics, such as drug loading ability, cytotoxicity, and degradability. Thus, it is of great significance to prepare size-customized PLGA-based NPs with a broad size range without varying the precursors, which could meet the different demands of NPs.

In contrast to conventional PLGA NPs preparation methods, such as emulsification–solvent evaporation, spray-drying, and phase separation, a microfluidic method produces size-controlled NPs with a narrow size distribution and good size batch-to-batch reproducibility[19–21]. Furthermore, using a solvent that is rapidly diluted with an aqueous solution in a microfluidic device, through varying flow conditions in microscale channels, enables the manipulation of nanoliter volumes, and the physicochemical features of the NPs can be controlled. In summary, the microfluidic method has enormous potential for substantiating size-controlled PLGA-based NPs.

At present, PLGA NPs with size control have been prepared using microfluidic methods[20–23]. However, size control over a wide range is achieved by changing the type of precursor. Unlike the nanoprecipitation method, Karnik *et al.* used a flow-focusing microfluidic device to mix miscible polymer solutions rapidly with water, and copolymers could self-assemble into formate NPs. By adding PLGA to poly (ethylene glycol) methyl ether block poly (lactic-co-glycolide) (PEG-PLGA) in different amounts,

NPs were prepared in the range of 30–105 nm[23]. Rhee *et al*. produced NPs with the average particle size of 30–230 nm mainly by modulating the molecular weight (27, 45, and 95 kDa) and varying concentration of PLGA from 10 to 50 mg/mL[20]; Valencia *et al.* designed devices with Tesla structures in microchannels to prepare NPs with the average particle size of 35–180 nm by changing the PLGA and DSPE-PEG composition and concentration of precursors[21]. If preparing a large range of size-controllable NPs without changing the polymer precursors is not achievable, finer customization, including the specified PLGA compound composition and controlled size of PLGA NPs, could not be allowed. To the best of our knowledge, no studies have been reported on manipulating the size-customized sub-200 nm PLGA-based NPs over a broad size range and with a good batch-to-batch repeatability without varying precursors.

In this study, we employed iLiNP®, designed by our group[24], to prepare a considerably wide variable nanoscale size range of PLGA-based NPs, without changing the polymer composition. Fig 2.1 shows a schematic of the iLiNP device. The prepared PLGA NPs exhibited excellent reproducibility and narrow size distribution. Owing to its latent capacity for medical application, paclitaxel (PTX) was employed as a model cancer therapy drug to be delivered with a high encapsulation efficiency (EE). Alternately, the cytotoxicity of different-sized PTX-loaded NPs *in vitro* was also investigated, which proved the potential capacity of the same composition PLGA size-controlled NPs within a wide size range in future DDS medical research.

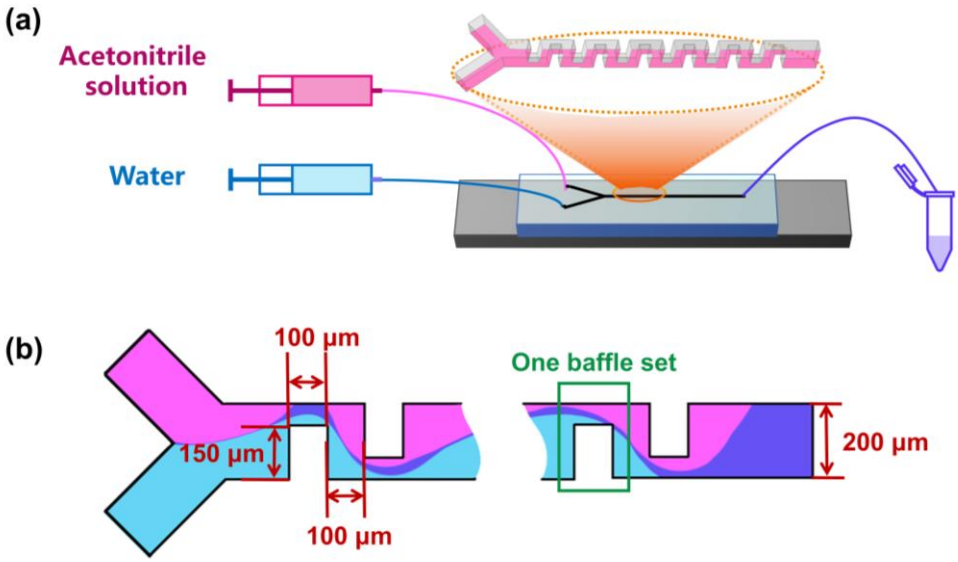

Fig 2.1 (a) Schematics of the iLiNP device to prepare blank or PTX-loaded NPs; (b) Top view of the iLiNP device. The width and depth of the channel were 200 and 100 μm, respectively. The device was equipped with 20 baffle sets

2.2 Materials and methods

2.2.1 Materials

PLGA (Mw = 24,000–38,000) and PEG-PLGA (average Mn_{PEG} = 2,000, average Mn_{PLGA} = 11,500) were purchased from Sigma–Aldrich (St. Louis, MO, USA). PTX was purchased from Tokyo Chemical Industry, Ltd. (Tokyo, Japan). Acetonitrile for the dissolving solvent and high-performance liquid chromatography (HPLC) was supplied by FUJIFILM Wako Pure Chemical Corporation (Osaka, Japan).

2.2.2 Fabrication of microfluidic devices

The design of the iLiNP device is illustrated in Fig 2.1. The width and depth of the channel were 200 μm and 100 μm, respectively. The polydimethylsiloxane (PDMS)-based iLiNP device was fabricated, followed by standard soft lithography[22], and bonded with a glass substrate to compose the iLiNP device. The detailed fabrication procedure of the iLiNP device has been reported previously[24].

2.2.3 Preparation of PLGA-based nanoparticles

The polymer (PLGA, PEG-PLGA, or blend [PLGA mixed with PEG-PLGA] with a mass ratio of 1:1) was dissolved in acetonitrile at different concentrations of 5 mg/mL. Then, PLGA/acetonitrile solution and ultrapure water (Milli Q; Direct-Q UV system, EMD Millipore Corporation, Billerica, MA, USA) were introduced into the iLiNP device from the two inlets. Two glass syringes (GASTIGHT 1002; Hamilton Inc., Reno, NV, USA) were filled with a polymer solution and ultrapure water, respectively. The syringes were connected to a microfluidic device, and syringe pumps (LEGATO 210; KD Scientific Inc., Holliston, MA, USA) were used to feed the solutions into the microfluidic device. After collecting the NPs in a microtube from the outlet, the solution was dialyzed in ultrapure water using a membrane tube (MWCO: 12–14 kD; Spectrum Laboratories, Inc., Canada) overnight at 4 °C. Finally, the size and stability of the NPs were evaluated using dynamic light scattering (DLS, Zetasizer Nano ZS ZEN3600; Malvern Instruments, UK).

For the conventional method, polymer (PLGA, PEG-PLGA, or blend [PLGA mixed with PEG-PLGA] with a mass ratio of 1:1) was dissolved in acetonitrile at 5 mg/mL concentration, and the polymer solution was added to ultrapure water using a

micropipette with stirring. The NP suspension was dialyzed overnight against ultrapure water.

When prepared using the chaotic mixer device, the method is similar to that of iLiNP. Briefly, the polymer (PLGA, PEG-PLGA, or blend [PLGA mixed with PEG-PLGA] with a mass ratio of 1:1) was dissolved in acetonitrile at a concentration of 5 mg/mL. The acetonitrile solution and ultrapure water in two syringes were then injected into the chaotic mixer device through two inlets using a syringe pump. The solution collected from the outlet would be dialyzed overnight in ultrapure water by the membrane tube.

2.2.4 Preparation of PTX-loaded nanoparticles and determination of drug content

Similar to the empty PLGA NPs, 5 mg/mL polymer and 0.5 mg/mL PTX (10% of polymer) were dissolved in acetonitrile, followed by introduction into the iLiNP device with ultrapure water from two different inlets. To remove the organic solvent and non-encapsulated drug, the collected solution was dialyzed overnight through the membrane tube in the ultrapure water. The PTX EE was determined using HPLC (L-2000 Elite LaChrom HPLC system; HITACHI, Japan). The NP solution was freeze-dried using freeze-drying equipment (Tokyo Rikakikai Co., Ltd., Japan), and the powder was dissolved in acetonitrile to dissolve the polymer and loaded PTX. The solution was filtered for HPLC analysis. A reverse-phase column (Shodex C18M 4D [inside diameter 150 × 4.6 mm, pore size 5 μm]; Shodex, Japan) was used to separate polymers and PTX, and the column temperature was maintained at 30 °C. The mobile phase consisted of acetonitrile/water (50:50 v/v) at a flow rate of 1.2 mL/min. PTX concentration was measured at a wavelength of 227 nm, and 20 μL of the sample was

injected using an autosampler. PTX solutions ranging from 5 to 100 μg/mL were prepared to construct a calibration curve. PTX EE was defined as the ratio of the amount of drug in the NPs to the initial amount of drug used for the preparation (Eq. (2.1)).

$$\text{Encapsulation Efficiency (EE\%)} = \frac{\text{Amount of PTX in nanoparticles}}{\text{The total amount of PTX}} \times 100\% \qquad (2.1)$$

2.2.5 Cytotoxicity studies

HeLa cells (kindly gifted by Dr. Yusuke Sato at Hokkaido University) were cultured in Dulbecco's modified Eagle's medium (DMEM, Sigma–Aldrich) supplemented with 10% fetal bovine serum (FBS) and 1% penicillin–streptomycin in an incubator with an atmosphere of 5% CO_2 and 37 °C. Blend-PTX NPs were prepared under concentration of 5 mg/mL blend (PLGA mixed with PEG-PLGA) with a mass ratio of 1:1 and 0.5 mg/mL PTX (10% of polymer). Two different sized blend-PTX were prepared with the flow condition as TFR is 50 μL/min or 500 μL/min, while the FRR is 3. After obtainting the EE of the NPs, blend-PTX NPs were

diluted to solutions of five different PTX concentrations by medium for cell uptake studies. Cytotoxic activity was evaluated using CellTiter-Blue (Promega, US) cell viability assay, and the steps are shown below.

Cells were seeded at a density of 5000 viable cells/well in 100 μL of the medium in a black 96-well microplate (Nunc, Denmark). The cells were then incubated with different concentrations of PTX in the medium solution or with different concentrations of PTX-loaded NPs. The microplates were incubated for 1, 2, or 3 d. After incubation, 20 μL CellTiter-Blue were added to each well, and the microplates were further incubated for 2 h. The fluorescence signal was measured using a fluorescence microplate reader at $560_{ex}/590_{em}$ nm. Cell viability was determined using Eq. (2.2)

$$\text{Cell viability (\%)} = \frac{A_{sample} - A_{negative}}{A_{positive} - A_{negative}} \times 100\% \quad (2.2)$$

where A_{sample}, $A_{negative}$, $A_{positive}$ are the fluorescence intensities of the sample, the negative control, and the positive control, respectively.

2.2.6 Statistical analysis

The results are expressed as mean ± standard deviation and analyzed using ANOVA to demonstrate statistical differences. The predictive value (P) ≤ 0.05 was considered statistically significant.

2.3 Results and discussion

2.3.1 Effect of the flow conditions on NP size

To investigate the effect of flow conditions on NP size, we introduced PLGA, PEG-PLGA, or blended (PLGA+PEG-PLGA, m_{PLGA}:$m_{PEG\text{-}PLGA}$ = 5:5) acetonitrile solution ($C_{polymer}$ = 5 mg/mL) with ultrapure water in the iLiNP device. The total flow rate (TFR) ranged from 50 to 500 μL/min, whereas the flow rate ratio (FRR) of aqueous phase to organic phase ranged from 3 to 9. Fig 2.2 and Fig 2.3 show the NP sizes and size distributions. In the case of lipid nanoparticles (LNPs), small-sized LNPs formed under high TFR and FRR conditions[24–27]. The PLGA NP size also decreased with an increase in the TFR, maintaining a single peak. NP sizes were 44–101 nm, 29–76 nm, and 40–114 nm for PLGA, PEG-PLGA, and blend NPs, respectively. With restriction to changing fluid conditions, only a narrow NP size range (23–29 nm under 50 mg/mL concentration or 20–26 nm at 20 mg/mL concentration) could be achieved by Karnik's method[23]. However, the FRR did not affect the NP size, which differs

from a previous study[23]. PEG-PLGA induced a decrease in NP size, similar to PEG-DMG, in the LNP system. Blend NPs showed the widest NP size range among the three polymers. We also evaluated the effect of the PLGA concentration, molecular weight, and PLGA composition on the NP size, polydispersity index (PDI) and NP stability (Fig 2.4-2.7, Table 2.1)

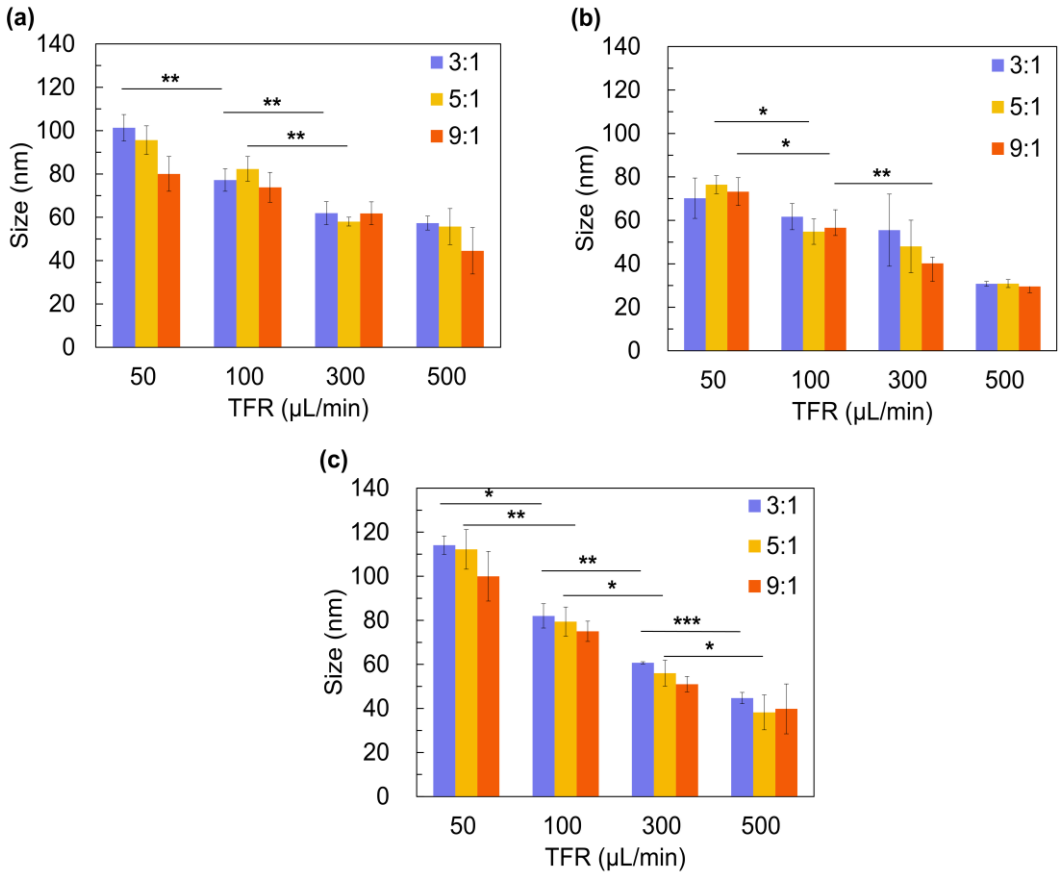

Fig 2.2 Effect of the flow condition on the NP size. (a) PLGA, (b) PEG-PLGA, and (c) blend. The FRR ranges from 3:1 to 9:1, whereas TFR ranges from 50 to 500 μL/min. The error bars represent the standard deviations calculated from the repeated NP preparation experiments at least three times. P-values: ***≤0.0001; **≤0.01, *<0.05

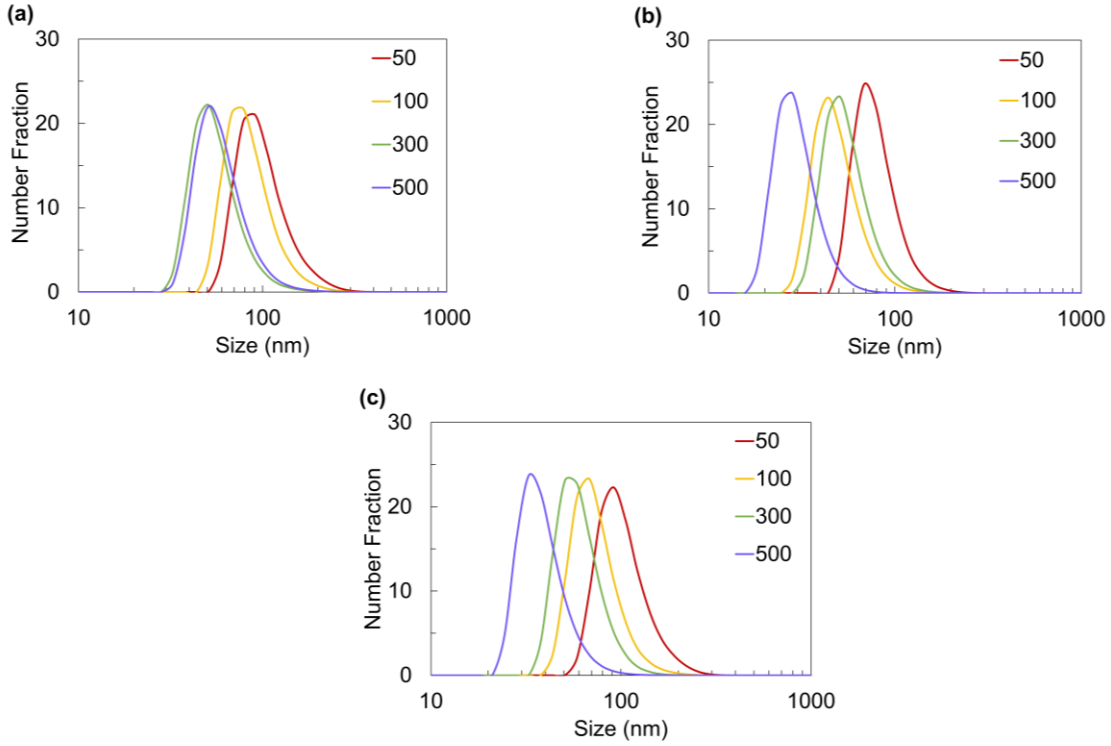

Fig 2.3 Size distribution of FRR = 5 with different TFR (μL/min). (a) PLGA, (b) PEG-PLGA, and (c) Blend.

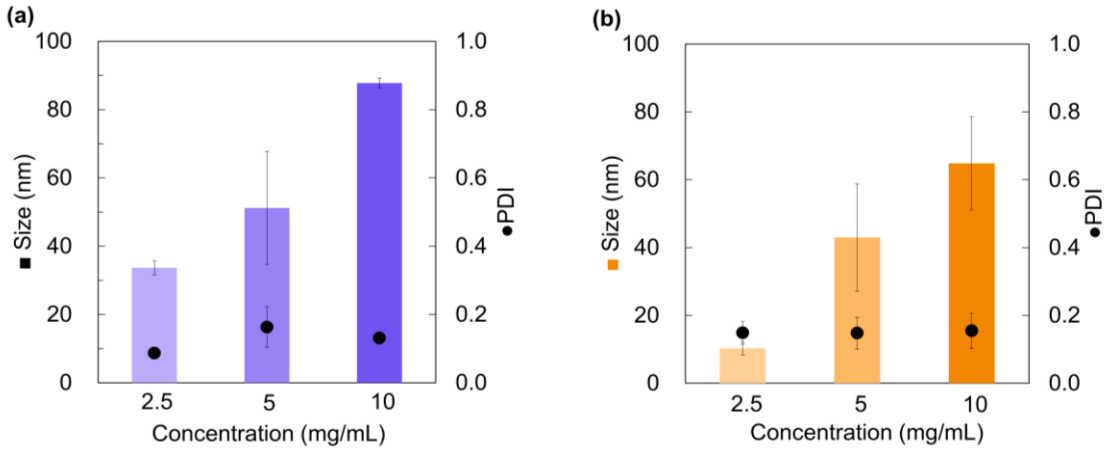

Fig 2.4 Effect of PLGA concentration. NPs were prepared at (a) TFR = 300 μL/min and (b) TFR = 500 μL/min. Concentration of PLGA acetonitrile solution varying from 2.5 to 10 mg/mL. The error bars represent the standard deviations calculated from repeated NP preparation experiments at least three times.

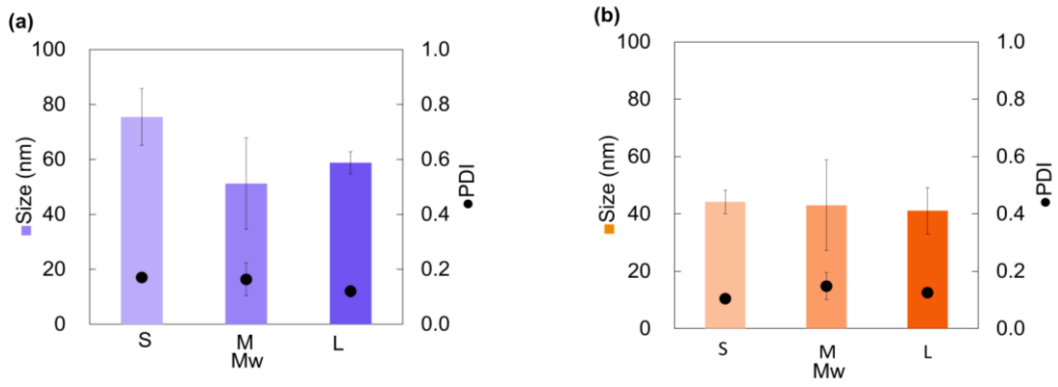

Fig 2.5 Effect of PLGA Mw. (a) TFR = 300 µL/min and (b) TFR = 500 µL/min.

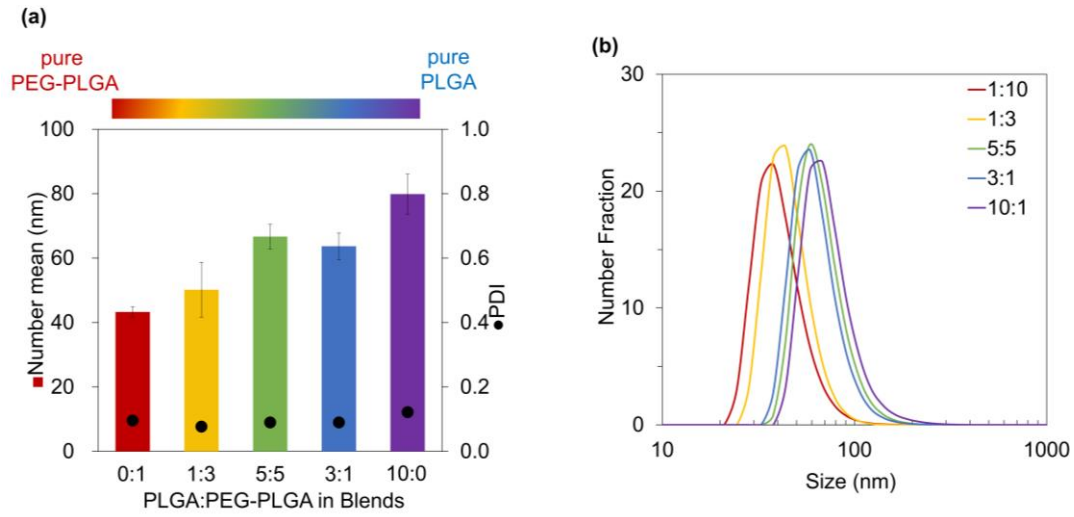

Fig 2.6 Effect of polymer composition. (a) Size and polydispersity index (PDI) comparison and (b) Size distribution with different PLGA:PEG-PLGA ratios. Data are presented as mean ± SEM; N > 3.

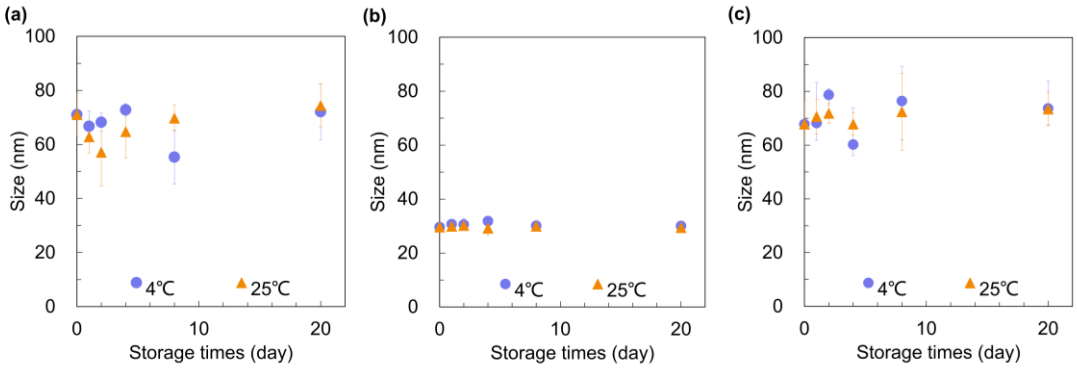

Fig 2.7 Evaluation of NP stability. (a) PLGA, (b) PEG-PLGA, and (c) blended NPs stored at 4 ℃ (purple dot) or 25 ℃ (orange dot). Data are presented as mean ± SEM; N = 3.

This NP formation behavior is probably due to the baffle structure of our device, w hich enables a far more effective solvent dilution performance than the sample flow-focusing device employed by Karnik. Based on the mechanism of self-assembly into microfluidic devices[23], the relationship between the solvent dilution time scale (τ_{mix}) and the polymer aggregation time scale (τ_{agg}) closely influences the size of the final NPs (Fig 2.8). In this study, the excellent solvent dilution performance allowed τ_{mix} to be much smaller than τ_{agg} in various FRR ranges. Therefore, polymer aggregation occurs when the solvent exchange is almost complete, and NP self-assembly occurs under conditions closer to the final solvent. Hence, the polymer does not readily assemble into NPs, resulting in smaller NPs. In contrast, the FRR change in this study cannot significantly affect the relationship between τ_{mix} and τ_{agg} and thus cannot significantly affect the NP size change. These results confirmed that the iLiNP device could control the NP size depending on the TFR without changing the precursors.

Table 2.1 Formulation code

Formulation code	
PLGA(S)	Mw = 7,000–17,000
PLGA(M)	Mw = 24,000–38,000
PLGA(L)	Mw = 38,000–54,000
PEG-PLGA	$n_{PEG} = n_{PLGA}$, average Mn_{PEG} = 2,000, average Mn_{PLGA} = 11,500
Blend (0:10)	$m_{PLGA(M)}:m_{PEG-PLGA}$ = 0:10
Blend (1:3)	$m_{PLGA(M)}:m_{PEG-PLGA}$ = 1:3
Blend (5:5)	$m_{PLGA(M)}:m_{PEG-PLGA}$ = 5:5
Blend (3:1)	$m_{PLGA(M)}:m_{PEG-PLGA}$ = 3:1
Blend (10:1)	$m_{PLGA(M)}:m_{PEG-PLGA}$ = 10:1

To study the effect of Mw, PLGA with Mw was dissolved in acetonitrile and introduced into the microfluidic device. Three types of PLGA were introduced: PLGA(S), PLGA(M), and PLGA(L) (S1 Table). The concentration of the PLGA acetonitrile solution used was 5 mg/mL. The TFR varied from 300 to 500 μL/min, and the FRR was 5. The PLGA NP size was not affected by Mw (Fig 2.5), which can be attributed to the aggregation of hydrophobic PLGA polymer into the microchannel or the effect of the dialysis process more than the difference in procurers.

We examined the effect of polymer composition on NPs using acetonitrile to dissolve different mass ratios of PLGA(M) with PEG-PLGA at 5 mg/mL concentration, TFR = 300 μL/min, and FRR = 5. The ratio of PLGA to PEG-PLGA ranged from 0:10 to 10:0; in this case, 0:10 indicates neat PEG-PLGA, and 10:0 indicates neat PLGA.

The NP size decreased from 80 ± 6 nm to 43 ± 2 nm with the increase in PEG-PLGA concentration in blends (Fig 2.6). This result may be attributed to the hydrophilic PEG blocks. Nucleation is achieved after the first stage of polymer self-assembly into

NPs, and the unimers add to the nucleus. Unlike neat PLGA, after the polymer brush layer is formed on the particle surface, the hydrophilic PEG block of PEG-PLGA acts as a shell of particles, which can increase the barrier to avoid aggregation; consequently, the size is smaller than that of the neat PLGA NPs. This result indicates that the polymer composition plays an important role in the preparation of small-sized NPs, which is consistent with other studies.

In addition to particle size and size distribution, the stability of NPs is significant both in vitro and in vivo. Ensuring the stability of the polymeric NPs during the long-term storage transportation would facilitate its effect. To check the stability of the NPs, the prepared PLGA NPs, PEG-PLGA NPs, and the blend were stored for 20 d at 4 ℃ and 25 ℃. The particle size was measured at predetermined time intervals. All NP types showed no significant differences during 20 d (Fig 2.7) and maintained a small size. In addition, NPs combined with PLGA showed slightly weaker stability than those without PLGA because the PEG layer acts as a shell around particles and reduces their interactions with foreign molecules, which can enhance the stability of particles. This result proved that the PLGA-based NPs prepared by the baffle device maintain high stability before uptake

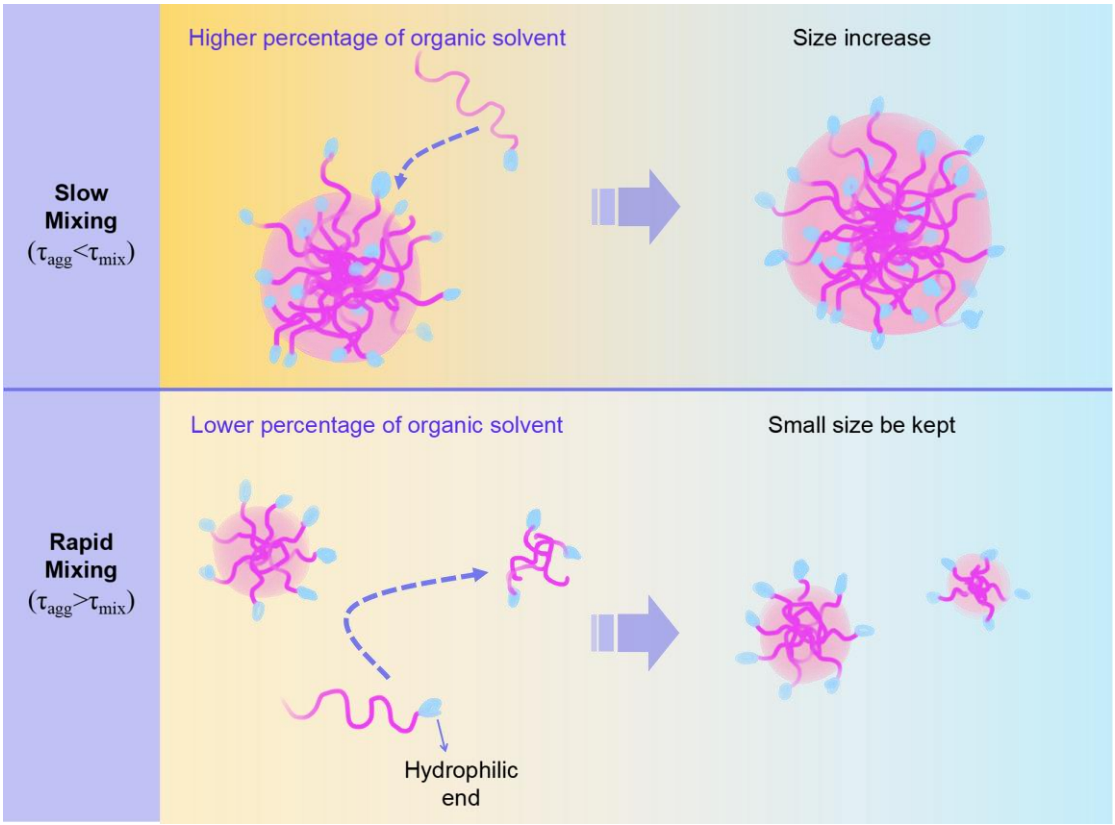

Fig 2.8 Mechanism of NP self-assembly during the solvent exchange. The relationship of the time scale of mixing and aggregation is the critical factor affecting the final particle size.

2.3.2 Comparison of the iLiNP device with the conventional method/chaotic mixer device

We compared the PLGA NP formation behavior using the iLiNP, the conventional method, and the chaotic mixer device with only varying flow conditions. Based on the adjustable particle size range of NPs prepared by the conventional method shown in Fig 2.9 (a) and the size range of NPs obtained from iLiNP preparation shown in Fig 2.2, we present the particle size range of the two methods as Fig 2.9 (b). From Fig 2.9 (b), it can be seen that the sizes of PLGA, PEG-PLGA, and blend NPs prepared by the

conventional method ranging 80–87 nm, 64–68 nm, and 81–90 nm, respectively, whereas the NP sizes prepared using the iLiNP device ranged from 44 to 101 nm, 29 to 76 nm, and 40 to 114 nm, respectively. In addition, the iLiNP device showed good NP size reproducibility compared with the conventional method. The iLiNP device enables the preparation of a larger range of particle sizes than conventional preparation methods. The difference in NP formation behavior may be attributed to the solvent dilution performance of the iLiNP device. In contrast, in the conventional method, it is difficult to precisely control the solvent dilution speed (stirring speed corresponding to the TFR in the microfluidic method) manually on a macroscopic scale. This observation shows that PLGA NPs prepared using the iLiNP device demonstrate better size controllability and a broader range of sizes than those prepared by the conventional methods, which could supply various demands when using the same polymer to prepare NPs with a broad size distribution.

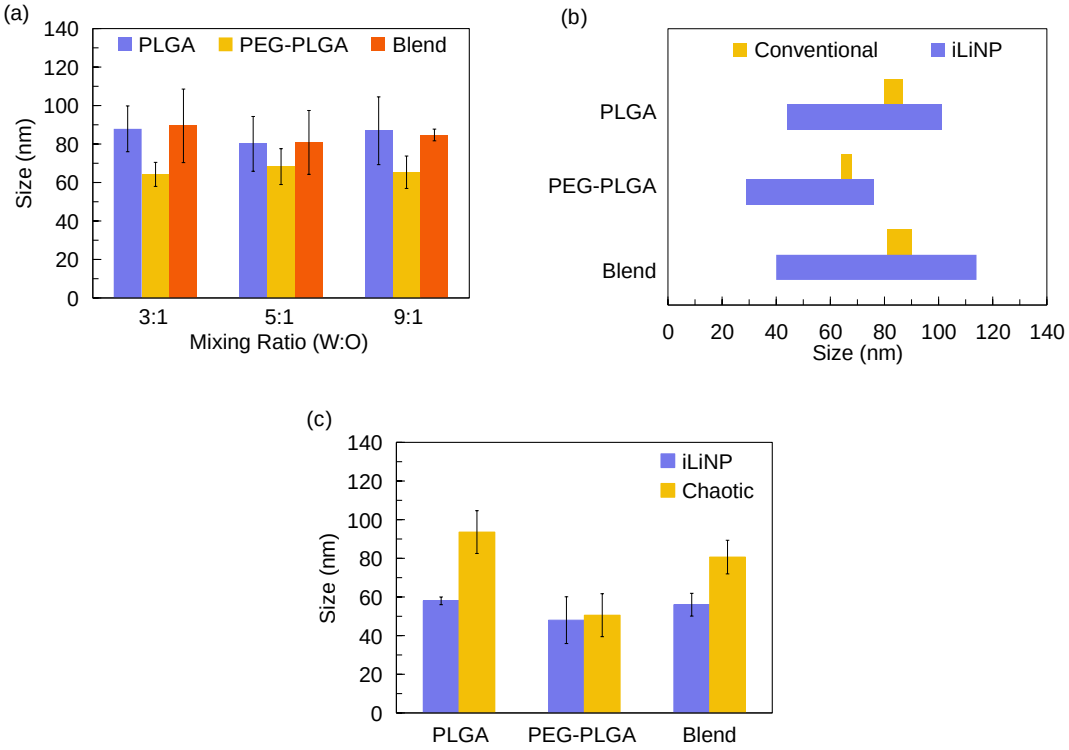

Fig 2.9 Comparison of NP sizes prepared using the iLiNP device, the chaotic mixer device, and the conventional method. (a) NP sizes prepared using the conventional method under different organic and aqueous solution ratios. The size range was: PLGA NPs: 80–87 nm; PEG-PLGA NPs: 64–68 nm; blend NPs: 81–90 nm; (b) Comparison of the particle size range of NPs prepared by the conventional method and the iLiNP device. (c) NP sizes prepared using the iLiNP device and the chaotic mixer device, NPs were prepared with FRR of 5 and TFR of 300 μL/min. The error bars represent the standard deviations calculated from the repeated NP preparation experiment more than three times.

The chaotic mixer device[28] can effectively mix the solutions in the microchannel. The PLGA, PEG-PLGA, or blend acetonitrile solution at 5 mg/mL concentration was introduced into the chaotic mixer device with a TFR of 300 μL/min and FRR of 5. Under the same flow condition, the NPs prepared using the chaotic device were larger

than those prepared using the iLiNP device, except PEG-PLGA NPs (Fig 2.9 (c)). Based on this mechanism (Fig 2.8), τ_{agg} was observed to be larger than τ_{mix} at rapid dilution.

Karnik et al. compared the zeta potential results of nanoparticles prepared using the bulk method with those of the microfluidic device method by adding PLGA to pure PEG-PLGA with altered precursors[23]. The results indicated that the zeta potential of nanoparticles prepared using the bulk method increased substantially with the addition of PLGA, whereas the microfluidic method did not. The PEG chain segments have negatively charged carboxyl terminals, and the increase in zeta potential indicates that fewer PEG chain segments are exposed on the particle surface. Furthermore, combined with the comparison of the TFR effect within the microfluidic device, during rapid dilution, the polymer molecules are located in the solution environment in which the amount of organic solvent is smaller than that of water. At this point, the hydrophilic chain segment is almost not present inside the particle, and the surface of the hydrophilic PEG surface barrier is sufficient, making the absorption or insertion of polymers into the NPs difficult. Moreover, the excess polymers must undergo more nucleation. The inverse of this theory shows that more efficient and rapid dilution can result in smaller particle sizes. In addition, the similar size of PEG-PLGA NPs prepared by the chaotic mixer device and the iLiNP is most likely due to the fact that the proportion of PEG segment components in PEG-PLGA is more than that of PLGA or blend. More PEG segment means easier to form PEG protective shells quickly (τ_{agg} of PEG-PLGA is different from that of PLGA or blend). It is known from the mechanism of polymer self-assembly that when enough hydrophilic chain segments form a protective shell on the outside, it will not be possible to make more polymers insert into the NPs, thus not leading to larger particle size. Under the flow rate conditions compared in this section, likely, the difference in mixing rate between the two

microfluidic devices at this time will not result in a significant change in the relationship between the τ_{agg} and τ_{mix} sizes of PEG-PLGA, and therefore the particle size will not change significantly.

In conclusion, these results demonstrate that the iLiNP device method can achieve a larger range of tunable NP size preparation than the bulk method and achieve rapid dilution of the organic solvent more efficiently than a typical microfluidic device chaotic mixer [24]. This finding demonstrates the superiority of this method and its great potential for further drug screening, custom drug delivery particle preparation, and other applications.

2.3.3 Drug loading into NPs

We loaded hydrophobic drugs into NPs using the iLiNP device and used PTX as a model drug. Fig 2.10 (a–c) shows a comparison between the average NP sizes of PTX-loaded NPs and unloaded-NPs prepared under different TFR conditions. Under the same flow condition of FRR = 3, PTX did not affect the NP size, regardless of the polymer type. The reproducibility of PTX-loaded NPs is slightly inferior to that of blank NPs (PTX-unloaded), which may be attributed to the hydrophobicity of PTX. The high hydrophobicity leads to more aggregation between particles during particle formation. This result proved that our method could be used to prepare blank and PTX-loaded NPs with a broad size range and good reproducibility. Moreover, the dependence of the PTX EE on the flow conditions and polymer composition was studied (Fig 2.10 (d)). The EE was ranged from 30% to 70%, depending on the polymer type. PTX loaded PLGA (PLGA-PTX NPs) prepared using microfluidic devices always show low EE and loading capacity, which is attributed to the large amounts of drugs lost during solvent displacement, while the NPs formed by the polymer chain come together. This due to

the principle of the continuous microfluidic method, which is the same as the solvent replacement method: while the preparation of drug-loaded PLGA NPs formed based on this principle, the drug is leaked out into the organic phase during solvent displacement[29–32]. Under the same polymer conditions, EE did not vary regularly with the TFR. Furthermore, the PTX-loaded blend (blend-PTX) NPs exhibited the highest EE among the three polymers. Compared to PTX-loaded PEG-PLGA (PEG-PLGA-PTX) NPs, the incorporation of PLGA increased EE, which is in agreement with a previous study[23]. This result is due to the hydrophobic PLGA increasing the hydrophobic core, thus improving the package capacity for the hydrophobic drug PTX. Meanwhile, PLGA-PTX NPs could not achieve a higher EE than blend-PTX NPs, which can be attributed to the lower PEG acting as hydrophobic layer protection for PLGA NPs. The loaded PTX, which is attached to the surface of PLGA NPs, is easily lost during the preparation process without the PEG brush barrier. Blend-PTX was selected for further *in vitro* experiments considering that blend-PTX NPs showed a larger NP size range than PLGA-PTX or PEG-PLGA-PTX NPs and enabled high EE.

2.3.4 *In vitro* antitumor activity

To demonstrate the effect of NP size on cytotoxicity, we prepared 52 nm and 109 nm-sized blend-PTX NPs (The blend-PTX NPs properties are consistent with those obtained for the preparation at 50 and 500 μL/min in Fig 2.10(c) (d)). Unlike other studies, the iLiNP device could control the NP size by TFR without changing the PLGA concentration, molecular weight, and composition. For the action mechanism of PTX, PTX binds microtubules and causes kinetic suppression of microtubule dynamics; thus, the cell cycle is consequently arrested at G2/M phases[33–35] We hypothesized that the NP size affects cellular uptake and PTX release kinetics and that this synergistic

effect would affect cytotoxicity. Free-PTX, 52 nm-sized PTX-loaded NPs, and 109 nm-sized PTX-loaded NPs were added to HeLa cells at different dosages. Fig 2.11 (a) shows the cell viability of free PTX unloaded into NPs. After 24 h, free PTX did not exhibit antitumor activity, regardless of the PTX concentration. Cell viability decreased to 50–80% and lower than 10% after 48 and 72 h of incubation, respectively. Fig 2.11 (b–c) shows the antitumor activity of 52 and 109 nm-sized NPs. Cytotoxicity of the blank NPs (PTX-unloaded) were shown in Fig 2.12. The blank blend NPs at 114 nm showed no toxicity from 0.1 μg/mL to 100 μg/mL, while the 45 nm blank blend NPs showed some toxicity to HeLa cells at higher concentrations. It has been previously reported that nano-sized PLGA particles can be toxic to cells to some extent[36,37]. After incubation with 52 nm blend-PTX for 24 h, cell viability remarkably reduced, whereas 109 nm blend-PTX could not show significant cytotoxicity. After 50 h of incubation, cell growth was almost completely inhibited by PTX-loaded NPs, regardless of NP size, and no significant difference was found in cytotoxicity among the different concentrations. Furthermore, after 72 h of incubation, all PTX-loaded NPs completely inhibited cell growth. Based on these results, it was observed that the blend-

PTX NPs with a 52 nm size could rapidly show high levels of antitumor activity compared to the 109 nm-sized NPs.

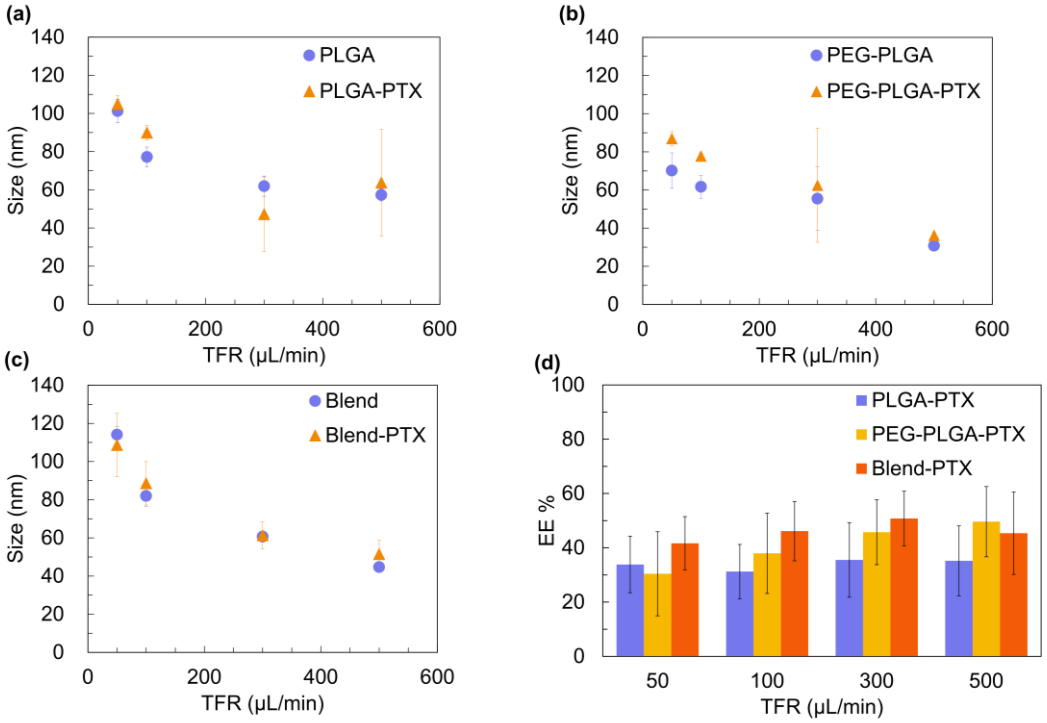

Fig 2.10 Size of blank NPs, PTX-loaded NPs, and EE of PTX. (a) PLGA NPs and PTX-loaded PLGA (PLGA-PTX) NPs; (b) PEG-PLGA NPs and PTX-loaded PEG-PLGA (PEG-PLGA-PTX) NPs; (c) blend NPs and PTX-loaded blend (blend-PTX) NPs. The purple dots represent blank NPs, and the orange dots are PTX-loaded NPs; (d) EE of PTX prepared at TFR of 50, 100, 300, and 500 μL/min and the FRR of 3. The error bars represent the standard deviations calculated from the repeated NP preparation experiment at least three times.

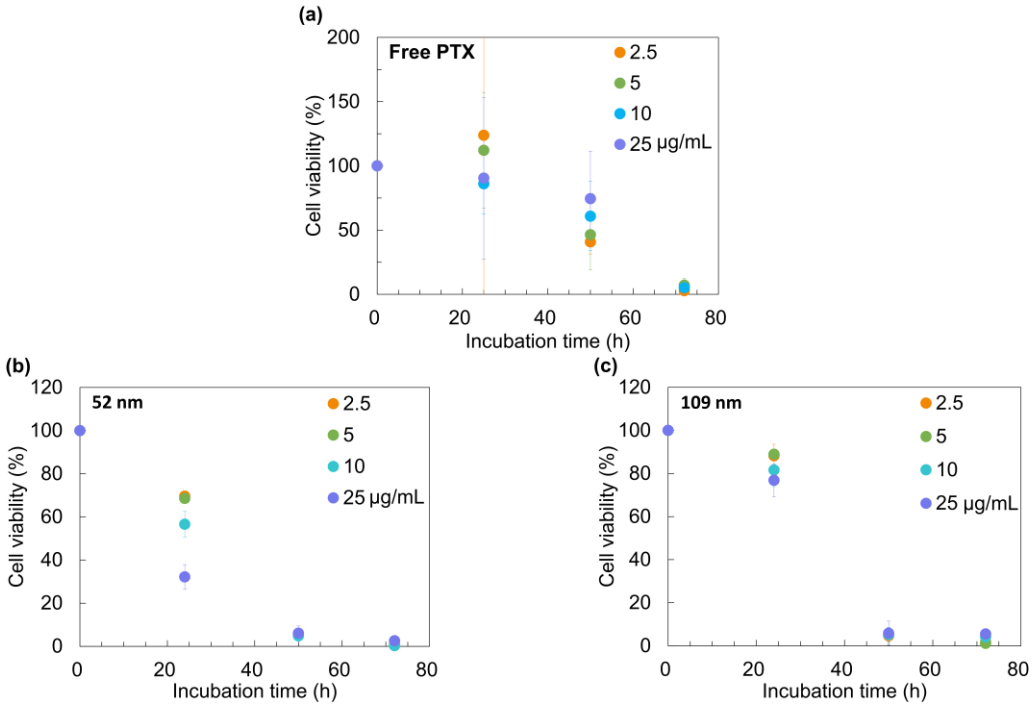

Fig 2.11 Cell viabilities dosed of (a) free-PTX, (b) 52 nm-sized blend-PTX NPs, and (c) 109 nm-sized blend-PTX NPs. Concentrations of PTX varied from 2.5 to 25 μg/mL. Preparation conditions for blend-PTX NPs: $C_{polymer}$= 5 mg/mL, TFR of 50 or 500 μL/min and the FRR of 3. The error bars represent the standard deviations calculated from the repeated NP preparation experiment at least three times.

Previous studies have shown that the cellular uptake of different kinds of NPs, such as gold NPs, silver NPs, and mesoporous silica NPs, by HeLa cells depends on their size, with the maximum uptake occurring at 50 nm[38–41]. However, as mentioned earlier, studies on Caco-2 cancer cells showed that small particle size (50 nm) had less cellular uptake than larger particle size[14,15]. In contrast, in KB cancer cells, small NP size (70 nm) had more cellular uptake than larger particles. This contrast is may be due to the different cell types, indicating that even for cancer cells, different cancer cell lines show different cellular uptake based on particle sizes. The effect of polymer NP size on the same precursor preparation of HeLa cells has not been

published, and our results precisely complement the research gap in this regard. In addition, our findings demonstrate a stronger case for providing a more finely size turnable PLGA NPs and satisfy the need to study the particle size effect and the mechanism behind it for targeted drug therapy.

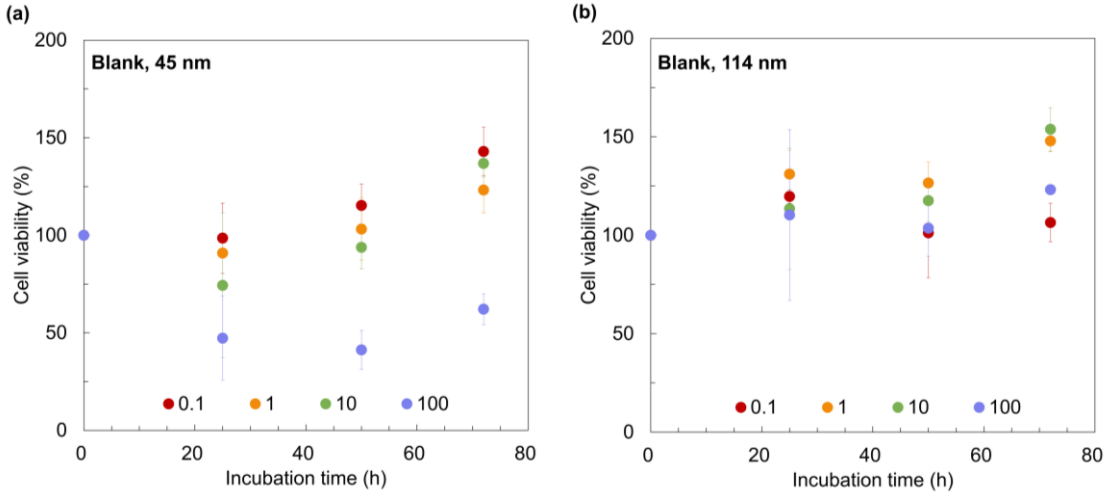

Fig 2.12 In *vitro* blank blended NP cell viability in HeLa cells. The blend concentration varying from 0.1 μg/mL to 100 μg/mL. (a) the average size of NPs is 45 nm, prepared at TFR = 500 μL/min. (b) the average size of NPs is 114 nm, prepared at TFR = 50 μL/min. Data are presented as mean ± SEM; N > 3.

2.4 Conclusion

In this study, size-tunable PLGA NPs were prepared using the iLiNP device. High flow rate produced small-sized NPs, whereas FRR did not markedly impact the size. In addition, the iLiNP device can prepare PLGA-based NPs with a broader size range (PLGA NPs: 44–101 nm; PEG-PLGA NPs: 29–76 nm; blend NPs: 40–114 nm) than those prepared using the conventional bulk method (PLGA NPs: 80–87 nm; PEG-PLGA NPs: 64–68 nm; blend NPs: 81–90 nm) and chaotic mixer device. In addition,

PTX was loaded into PLGA/PEG-PLGA/blend NPs. We found that 52 nm-sized PTX-loaded NPs inhibited cell growth and showed higher antitumor activity than 109 nm sized NPs. The NPs were prepared using the same polymer solution under different TFR conditions. An NP size-tunable technique without any optimization of molecular weight, concentration, and composition of the polymer is crucial for developing DDS nanomedicines. We believe that iLiNP-based polymer-based NP production will provide abundant possibilities for future clinical applications of size-controlled nanomedicines

References

1. Riehemann K, Schneider SW, Luger TA, Godin B, Ferrari M, Fuchs H. Nanomedicine - Challenge and perspectives. Angewandte Chemie - International Edition. 2009;48: 872–897. doi:10.1002/anie.200802585
2. Lepeltier E, Bourgaux C, Couvreur P. Nanoprecipitation and the “Ouzo effect”: Application to drug delivery devices. Advanced Drug Delivery Reviews. Elsevier; 2014. pp. 86–97. doi:10.1016/j.addr.2013.12.009
3. Wilczewska AZ, Niemirowicz K, Markiewicz KH. Nanoparticles as drug delivery systems. Pharmacological reports. 2012;64: 1020–1037. doi:10.1016/S1734-1140(12)70901-5
4. Panyam J, Labhasetwar V. Biodegradable nanoparticles for drug and gene delivery to cells and tissue. Advanced Drug Delivery Reviews. 2003;55: 329–347. doi:10.1016/S0169-409X(02)00228-4
5. Giteau A, Venier-Julienne MC, Aubert-Pouëssel A, Benoit JP. How to achieve sustained and complete protein release from PLGA-based microparticles? International Journal of Pharmaceutics. Elsevier; 2008. pp. 14–26. doi:10.1016/j.ijpharm.2007.11.012
6. Cruz LJ, Tacken PJ, Fokkink R, Joosten B, Stuart MC, Albericio F, et al. Targeted PLGA nano- but not microparticles specifically deliver antigen to human dendritic cells via DC-SIGN in vitro. Journal of Controlled Release. 2010;144: 118–126. doi:10.1016/j.jconrel.2010.02.013
7. Cun D, Jensen DK, Maltesen MJ, Bunker M, Whiteside P, Scurr D, et al. High loading efficiency and sustained release of siRNA encapsulated in PLGA nanoparticles: Quality by design optimization and characterization. European Journal of Pharmaceutics and Biopharmaceutics. 2011;77: 26–35. doi:10.1016/j.ejpb.2010.11.008
8. Makadia HK, Siegel SJ. Poly Lactic-co-Glycolic Acid (PLGA) as Carrier. Polymers. 2011;3: 1377–1397. doi:10.3390/polym3031377
9. Martínez Rivas CJ, Tarhini M, Badri W, Miladi K, Greige-Gerges H, Nazari QA, et al. Nanoprecipitation process: From encapsulation to drug delivery. International Journal of Pharmaceutics. 2017;532: 66–81. doi:10.1016/J.IJPHARM.2017.08.064

10. Sharma S, Parmar A, Kori S, Sandhir R. PLGA-based nanoparticles: A new paradigm in biomedical applications. TrAC Trends in Analytical Chemistry. 2016;80: 30–40. doi:10.1016/J.TRAC.2015.06.014
11. Ananta JS, Paulmurugan R, Massoud TF. Temozolomide-loaded PLGA nanoparticles to treat glioblastoma cells: a biophysical and cell culture evaluation. Neurological research. 2016;38: 51–59. doi:10.1080/01616412.2015.1133025
12. Danhier F, Lecouturier N, Vroman B, Jérôme C, Marchand-Brynaert J, Feron O, et al. Paclitaxel-loaded PEGylated PLGA-based nanoparticles: In vitro and in vivo evaluation. Journal of Controlled Release. 2009;133: 11–17. doi:10.1016/j.jconrel.2008.09.086
13. Choi JS, Cao J, Naeem M, Noh J, Hasan N, Choi HK, et al. Size-controlled biodegradable nanoparticles: Preparation and size-dependent cellular uptake and tumor cell growth inhibition. Colloids and Surfaces B: Biointerfaces. 2014;122: 545–551. doi:10.1016/J.COLSURFB.2014.07.030
14. Xu A, Yao M, Xu G, Ying J, Ma W, Li B, et al. A physical model for the size-dependent cellular uptake of nanoparticles modified with cationic surfactants. International Journal of Nanomedicine. 2012;7: 3547–3554. doi:10.2147/IJN.S32188
15. Yin Win K, Feng S-S. Effects of particle size and surface coating on cellular uptake of polymeric nanoparticles for oral delivery of anticancer drugs. Biomaterials. 2005;26: 2713–2722. doi:10.1016/j.biomaterials.2004.07.050
16. Singh R, Lillard Jr JW. Nanoparticle-based targeted drug delivery. Experimental and Molecular Pathology. 2009;86: 215–223. doi:10.1016/j.yexmp.2008.12.004
17. Kreuter J, Ramge P, Petrov V, Hamm S, Gelperina SE, Engelhardt B, et al. Direct Evidence That Polysorbate-80-Coated Poly(Butylcyanoacrylate) Nanoparticles Deliver Drugs to the CNS via Specific Mechanisms Requiring Prior Binding of Drug to the Nanoparticles. Pharmaceutical Research. 2003;20: 409–416. doi:10.1023/A:1022604120952
18. Cabral H, Matsumoto Y, Mizuno K, Chen Q, Murakami M, Kimura M, et al. Accumulation of sub-100 nm polymeric micelles in poorly permeable tumours depends on size. Nature Nanotechnology. 2011;6: 815–823. doi:10.1038/nnano.2011.166

19. Damiati S, Kompella UB, Damiati SA, Kodzius R. Microfluidic devices for drug delivery systems and drug screening. Genes. MDPI AG; 2018. p. 103. doi:10.3390/genes9020103
20. Rhee M, Valencia PM, Rodriguez MI, Langer R, Farokhzad OC, Karnik R. Synthesis of Size-Tunable Polymeric Nanoparticles Enabled by 3D Hydrodynamic Flow Focusing in Single-Layer Microchannels. Advanced Materials. 2011;23: H79–H83. doi:10.1002/adma.201004333
21. Valencia PM, Basto PA, Zhang L, Rhee M, Langer R, Farokhzad OC, et al. Single-Step Assembly of Homogenous Lipid−Polymeric and Lipid−Quantum Dot Nanoparticles Enabled by Microfluidic Rapid Mixing. ACS Nano. 2010;4: 1671–1679. doi:10.1021/nn901433u
22. Sia SK, Whitesides GM. Microfluidic devices fabricated in poly(dimethylsil-oxane) for biological studies. Electrophoresis. 2003;24: 3563–3576. doi:10.1002/elps.200305584
23. Karnik R, Gu F, Basto P, Cannizzaro C, Dean L, Kyei-Manu W, et al. Microfluidic Platform for Controlled Synthesis of Polymeric Nanoparticles. Nano Letters. 2008;8: 2906–2912. doi:10.1021/nl801736q
24. Kimura N, Maeki M, Sato Y, Note Y, Ishida A, Tani H, et al. Development of the iLiNP Device: Fine Tuning the Lipid Nanoparticle Size within 10 nm for Drug Delivery. ACS Omega. 2018;3: 5044–5051. doi:10.1021/acsomega.8b00341
25. Maeki M, Saito T, Sato Y, Yasui T, Kaji N, Ishida A, et al. A strategy for synthesis of lipid nanoparticles using microfluidic devices with a mixer structure. RSC Advances. 2015;5: 46181–46185. doi:10.1039/C5RA04690D
26. Maeki M, Uno S, Niwa A, Okada Y, Tokeshi M. Microfluidic technologies and devices for lipid nanoparticle-based RNA delivery. Journal of Controlled Release. 2022;344: 80–96. doi:10.1016/J.JCONREL.2022.02.017
27. Maeki M, Okada Y, Uno S, Niwa A, Ishida A, Tani H, et al. Production of siRNA-Loaded Lipid Nanoparticles using a Microfluidic Device. Journal of visualized experiments. 2022; e62999. doi:10.3791/62999
28. Stroock AD, Dertinger SKW, Ajdari A, Mezić I, Stone HA, Whitesides GM. Chaotic mixer for microchannels. Science. 2002;295: 647–651. doi:10.1126/science.1066238

29. Fessi H, Puisieux F, Devissaguet JP, Ammoury N, Benita S. Nanocapsule formation by interfacial polymer deposition following solvent displacement. International Journal of Pharmaceutics. 1989;55: R1–R4. doi:10.1016/0378-5173(89)90281-0
30. Su Y, Liu J, Tan S, Liu W, Wang R, Chen C, et al. PLGA sustained-release microspheres loaded with an insoluble small-molecule drug: microfluidic-based preparation, optimization, characterization, and evaluation in vitro and in vivo. https://doi.org/101080/1071754420222072413. 2022;29: 1437–1446. doi:10.1080/10717544.2022.2072413
31. Niwa T, Takeuchi H, Hino T, Kunou N, Kawashima Y. Preparations of biodegradable nanospheres of water-soluble and insoluble drugs with D,L-lactide/glycolide copolymer by a novel spontaneous emulsification solvent diffusion method, and the drug release behavior. Journal of Controlled Release. 1993;25: 89–98. doi:10.1016/0168-3659(93)90097-O
32. Barichello JM, Morishita M, Takayama K, Nagai T. Encapsulation of hydrophilic and lipophilic drugs in PLGA nanoparticles by the nanoprecipitation method. Drug Development and Industrial Pharmacy. 1999;25: 471–476. doi:10.1081/DDC-100102197
33. Jordan MA, Wilson L. Microtubules and actin filaments: Dynamic targets for cancer chemotherapy. Current Opinion in Cell Biology. 1998;10: 123–130. doi:10.1016/S0955-0674(98)80095-1
34. Schiff PB, Horwitz SB. Taxol stabilizes microtubules in mouse fibroblast cells. Proceedings of the National Academy of Sciences of the United States of America. 1980;77: 1561–1565. doi:10.1073/pnas.77.3.1561
35. Jordan MA, Toso RJ, Thrower D, Wilson L. Mechanism of mitotic block and inhibition of cell proliferation by taxol at low concentrations. Proceedings of the National Academy of Sciences of the United States of America. 1993;90: 9552–9556. doi:10.1073/pnas.90.20.9552
36. Dunn SS, Luft JC, Parrott MC. Zapped assembly of polymeric (ZAP) nanoparticles for anti-cancer drug delivery. Nanoscale. 2019;11: 1847–1855. doi:10.1039/C8NR09944H
37. Ibrahim WN, Rosli LMBM, Doolaanea AA. Formulation, Cellular Uptake and Cytotoxicity of Thymoquinone-Loaded PLGA Nanoparticles in Malignant

Melanoma Cancer Cells. International Journal of Nanomedicine. 2020;15: 8059. doi:10.2147/IJN.S269340

38. Chithrani BD, Ghazani AA, Chan WCW. Determining the size and shape dependence of gold nanoparticle uptake into mammalian cells. Nano Letters. 2006;6: 662–668. doi:10.1021/nl052396o

39. Lu F, Wu S-H, Hung Y, Mou C-Y. Size Effect on Cell Uptake in Well-Suspended, Uniform Mesoporous Silica Nanoparticles. Small. 2009;5: 1408–1413. doi:10.1002/smll.200900005

40. Jiang W, Kim BYS, Rutka JT, Chan WCW. Nanoparticle-mediated cellular response is size-dependent. Nature Nanotechnology. 2008;3: 145–150. doi:10.1038/nnano.2008.30

41. Osaki F, Kanamori T, Sando S, Sera T, Aoyama Y. A quantum dot conjugated sugar ball and its cellular uptake. On the size effects of endocytosis in the subviral region. Journal of the American Chemical Society. 2004;126: 6520–6521. doi:10.1021/ja048792a

CHAPTER 3 Effect of organic solvents on the production of PLGA-based drug-loaded nanoparticles using a microfluidic device

3.1 Introduction

The advent of nanoparticles (NPs) has helped to successfully overcome the inadequacies of conventional drug delivery systems (DDS); they have proven to be powerful weapons against a wide range of diseases[1,2]. NPs have been used to overcome numerous treatment obstacles[3],[4]. They have demonstrated improved permeability, bioavailability, drug pharmacokinetics, stability in biological matrices, reduced adverse effects, and other features when used for drug administration[5–9]. Poly(lactic-co-glycolic-acid) (PLGA) polymeric NPs, in particular, are FDA-approved polymers and one of the most extensively utilized polymers in the development of nanomedicines because of their high structural integrity, tunable properties, and versatility in surface functionalization and stability[10–12]. Different functionalized innovative PLGA NPs that can target fatal cancer cells have been reported in various studies[13–16]. However, only a few formulations have been transformed into clinical applications, and only a handful have a substantial impact. Part of the challenge lies in the complexity of optimizing the NPs, because the optimal NPs parameters (surface charge, particle size, surface roughness, *etc*.) need to be determined according to different disease types and lesion locations[17]. In other words, to obtain finely customized DDS and tailored medications, there is still a long way to go.

The size-dependent cell uptake in different cell lines have been widely demonstrated[18–22], and this has greatly encouraged the advancement of size-targeted therapeutic regimens via precise particle size modulation. Microfluidic devices can precisely modulate minimal fluid volumes in microscale-controlled channels to prepare particles with controlled sizes and great batch-to-batch reproducibility[23–30]. Furthermore, microfluidic-based nanoprecipitation

allows the use of expensive therapeutics in small volumes to screen different experimental conditions and to develop optimal formulations of NP-based nanomedicines. For the preparation of PLGA NPs using the nanoprecipitation method, the solvent effect is a significant factor in controlling the NP size and encapsulating hydrophobic drugs. In particular, tetrahydrofuran (THF) is widely used as a solvent to dissolve various hydrophobic materials[31]. Therefore, in the microfluidic-based nanoprecipitation method, the use of THF as the solvent can expand NP design, including hydrophobic drug encapsulation and modification of NPs with hydrophobic materials[32–34].

Polydimethylsiloxane (PDMS) is one of the most widely used materials in microfluidic devices[17]. However, due to the restrictive nature of PDMS, it cannot be applied to a wide range of organic reagents because of the swelling of the solvent[35,36]. Therefore, only few studies have focused on comparing the effect of solvents on the preparation of PLGA NPs in microfluidic devices. Understanding the effect of solvents, including THF, on PLGA NP size is essential for the development of novel PLGA-based nanomedicines.

In this study, we investigated the effects of organic solvents on the size of PLGA-NPs using a glass-based microfluidic device. Using the glass-based microfluidic device, it was possible to first evaluate the PLGA NP production behavior in the microchannel. In addition, to verify the feasibility of diverse drug encapsulation screens, we employed three distinct forms of taxanes (paclitaxel [PTX], cabazitaxel [CTX], and docetaxel [DTX]) as model drugs for encapsulation and evaluated *in vitro* experimental results. The prepared NPs maintained good batch-to-batch reproducibility and size-dependent cytotoxicities. The glass-based microfluidic device enables rapid optimization and screening of more favorable conditions for the

preparation of NPs for DDS, accelerates clinical drug screening, and has the potential to assist rapid transfer to preclinical investigations.

3.2 Experimental

3.2.1 Materials

PLGA (50:50 ratio, Mw = 24000–38000 Da) and PEG-PLGA (average Mn_{PEG} = 2000 Da, average Mn_{PLGA} = 11500 Da) were obtained from Sigma–Aldrich (St. Louis, MO, USA). PTX, COX, and DOX were purchased from Tokyo Chemical Industry Ltd. (Tokyo, Japan). Acetonitrile (ACN), dimethyl sulfoxide (DMSO), dimethylformamide (DMF), and tetrahydrofuran (THF) were purchased from FUJIFILM Wako Pure Chemical Corporation (Osaka, Japan).

3.2.2 Preparation of polymeric NPs

A 5 mg/mL mixture of PLGA and PEG-PLGA with a mass ratio of 1:1, and 0.5 mg/mL of different kinds of anti-cancer drugs (10% of polymer) were dissolved in an organic solvent. The syringes were connected to the microfluidic device, and the organic solution was fed with ultrapure water into the microfluidic device from two different inlets using syringe pumps (LEGATO 210; KD Scientific Inc., Hollistion, MA, USA). The collected solution was dialyzed overnight in ultrapure water through a membrane bag (MWCO:12-14kD; Spectrum Laboratories, Inc., Canada) to remove the organic solvent. The sizes of the NPs were evaluated using dynamic light scattering (DLS. Zetasizer nano ZS ZEN360; Malvern Instruments, UK).

3.2.3 Determination of the encapsulation efficiency

The drug content of the NPs was determined using HPLC (HITACHI, Japan). The NPs solution was freeze-dried to a powder, which was then dissolved in ACN. For PTX and DTX, the mobile phase consisted of ACN and water (50:50 v/v) and a reverse-phase column was used to maintain a temperature of 30 °C. The flow rate was 1.2 mL/min and the UV detection wavelength was 227 nm. CTX was ACN: water = 58:42 (v/v), the flow rate was 1.0 mL/min and the UV detection wavelength was 228 nm.

The HPLC was calibrated using a standard solution containing 5–100 μg/mL of the drug in CAN (Fig 3.1). The encapsulation efficiency (EE) can be determined by the ratio of the amount of drug inside the sample solution to the amount of drug used for NPs preparation (Eq. (3.1))

$$\text{EE}\ (\%) = \frac{\text{Amount of drugs in NPs}}{\text{The total amount of drug}} \times 100\% \qquad (3.1)$$

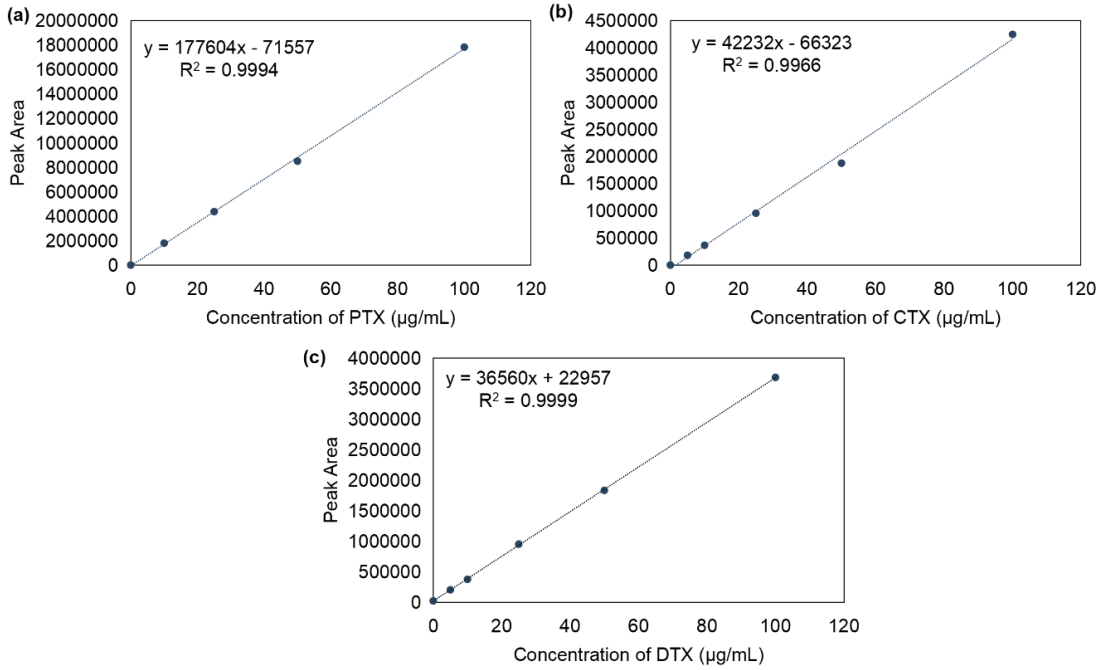

Fig 3.1 Standard curve for drug determined by HPLC. (a) PTX; (b) CTX; (c) DTX.

3.2.4 Cell viability

Human cervical cancer HeLa cells were grown in Dulbecco's modified essential medium (DMEM, Sigma-Aldrich, St. Louis, MO, USA) supplemented with 10% (v/v) fetal bovine serum (FBS) and 1% penicillin-streptomycin. The cells were maintained in a humidified atmosphere containing 5% CO_2 at 37 °C in an incubator.

The cells were seeded in 96-well plates at a density of 5000 cells/well. After the cells adhered to the wall of the plate, NPs were added and incubated with at least three replicate wells per group for a certain period. After incubation, cytotoxicity was assayed by adding 10 μL of Cell Counting kit-8 (CCK-8, Dojindo, Japan) solution. The plates were further incubated for 1 h before measuring absorbance at 450 nm using a microplate reader (Infinite-M Nano 200 Pro, TECAN, Switzerland). Equation (3.2) was employed to determine cell viability.

$$\text{Cell viability (\%)} = \frac{A_{sample} - A_{negative}}{A_{positive} - A_{negative}} \times 100\% \quad (3.2)$$

where A_{sample}, $A_{positive,}$ and $A_{negetive}$ are the absorbance of the sample, positive control, and negative control, respectively.

3.2.5 Statistical analysis

The results are expressed as the mean ± standard deviation and were analyzed using T-TEST to demonstrate statistical differences. A predictive value (P) $\leqslant$ 0.05 was statistically significant.

3.3 Results and discussion

3.3.1 Effect of the flow condition on the PLGA NP size

Fig 3.2 shows an illustration and a photograph of the microfluidic device used for PLGA NP production. The structure of the glass-based microfluidic device was based on a previous study, and it was obtained from Shin-Etsu Chemical Co., Ltd.. Here, microfluidic channels are realized by the soft chemical etching method[37,38].

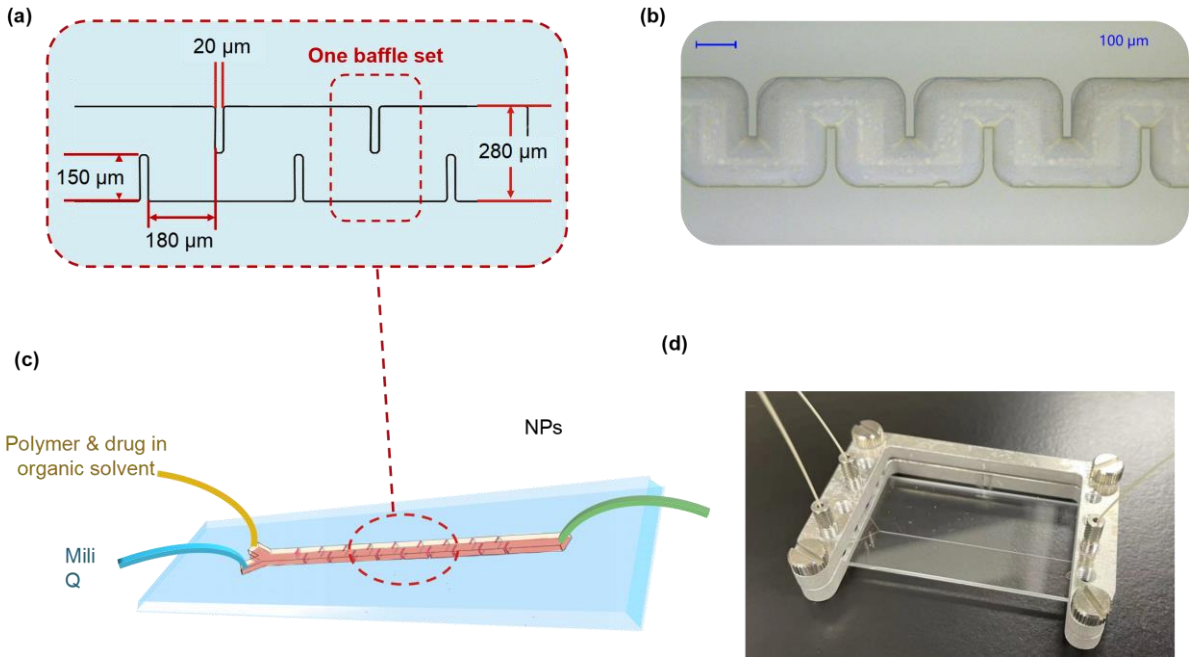

Fig 3.2 (a) Top view of the glass-based microfluidic device. The depth of the channel was 60 μm. The device was equipped with 20 baffle sets; (b) Microscope image of the glass device; (c) Schematics of the PLGA-based NPs preparation using the glass device; (d) Picture of glass device.

To evaluate the NP size controllability of the glass device, we produced PLGA NPs using acetonitrile as the solvent. Fig 3.3(a) shows the PLGA NP sizes produced at the total flow rate

(TFR) of 50, 500, and 1000 μL/min using a flow rate ratio (FRR; aqueous phase/organic phase) of 3. The NP size decreased from 146 nm to 37 nm when the TFR was increased from 50 to 1000 μL/min, and the NPs were able to maintain a good polydispersity index (PDI) under all flow conditions (Fig 3.3(a)). This was attributed to the more rapid solvent exchange process described in the previous work[39]. This result implies that the glass device can tolerate a higher TFR and can prepare monodisperse particles with high reproducibility in this flow rate range. As shown in Fig 3.3(b), the NPs prepared with the glass device were larger than those obtained with the PDMS device under the same flow conditions; this was due to the difference in the microchannels caused by the device fabrication process (Fig 3.3(c)). The solvent exchange performance of the glass device was reduced compared to that of the PDMS device due to its wide microchannel structure. Overall, the results imply that the glass device can tolerate a higher TFR. Additionally, the PLGA NPs prepared by glass devices are monodisperse and enable high reproducibility.

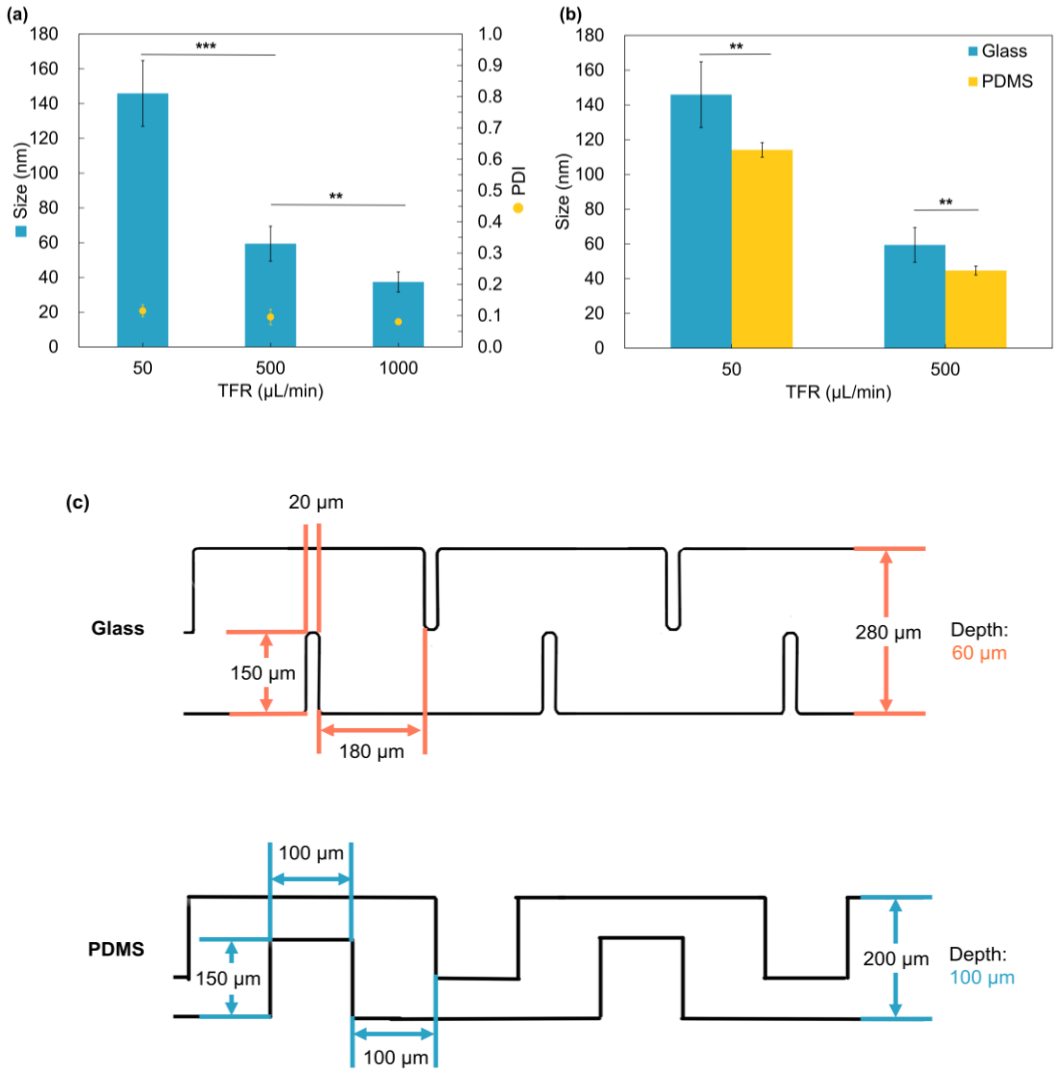

Fig 3.3 (a) Effect of the flow condition on PLGA NPs size in the glass device. (b) Difference between NPs prepared by the glass and PDMS microfluidic devices. (c) Comparison of the design of glass and PDMS devices. The NPs were prepared by dissolving polymers in acetonitrile at FRR 3. The standard deviations from the repeated preparation experiments were more than 3 times. P-values: ***≤0.0001; **≤0.001, *≤0.05.

3.3.2 Effect of solvent properties on the PLGA NP size

The properties of the organic solvent affect the diffusion of the organic and aqueous phases within the microchannel, thus causing a variation in the solvent exchange time. In addition, solvent polarity is a major factor in the nanoprecipitation method used to control the NP size[31,40,41]. However, PDMS cannot use various solvents, particularly low-polarity solvents, owing to the swelling of PDMS[35]. In contrast to the PDMS device, the glass device showed high chemical resistance and could use low-polarity solvents. We conducted experiments using acetonitrile (ACN), dimethyl sulfoxide (DMSO), dimethylformamide (DMF), and THF, which are miscible with water. The important physicochemical parameters of these solvents are listed in Table 1 and are relevant for the discussion of the experimental data.

Table 3.1 Properties of organic solvents.

	Molecular formulas	Viscosity at 25℃ (cap)	Surface Tension (N/m)	Hildebrand solubility parameter ($MPa^{1/2}$)	Polarity Index
ACN	C_2H_3N	0.34	28.7	24.3	5.8
DMSO	C_2H_6OS	1.97	42.9	26.7	7.2
DMF	C_3H_7NO	0.80	36.4	24.8	6.4
THF	C_4H_8O	0.46	27.1	18.5	4.0
Water	H_2O	0.89	72	47.9	10.2

As shown in Fig 3.4, PLGA NP formation behavior using ACN and THF was similar, and monodisperse NPs were prepared at flow rates of 50 or 500 μL/min with good reproducibility.

However, DMF and DMSO could only achieve the formation of monodispersed NPs at a low flow rate of 50 µL/min. Polydisperse NPs were formed at a TFR of 500 µL/min. The solvent parameters listed in Table 3.1 were related to the particle size formation.

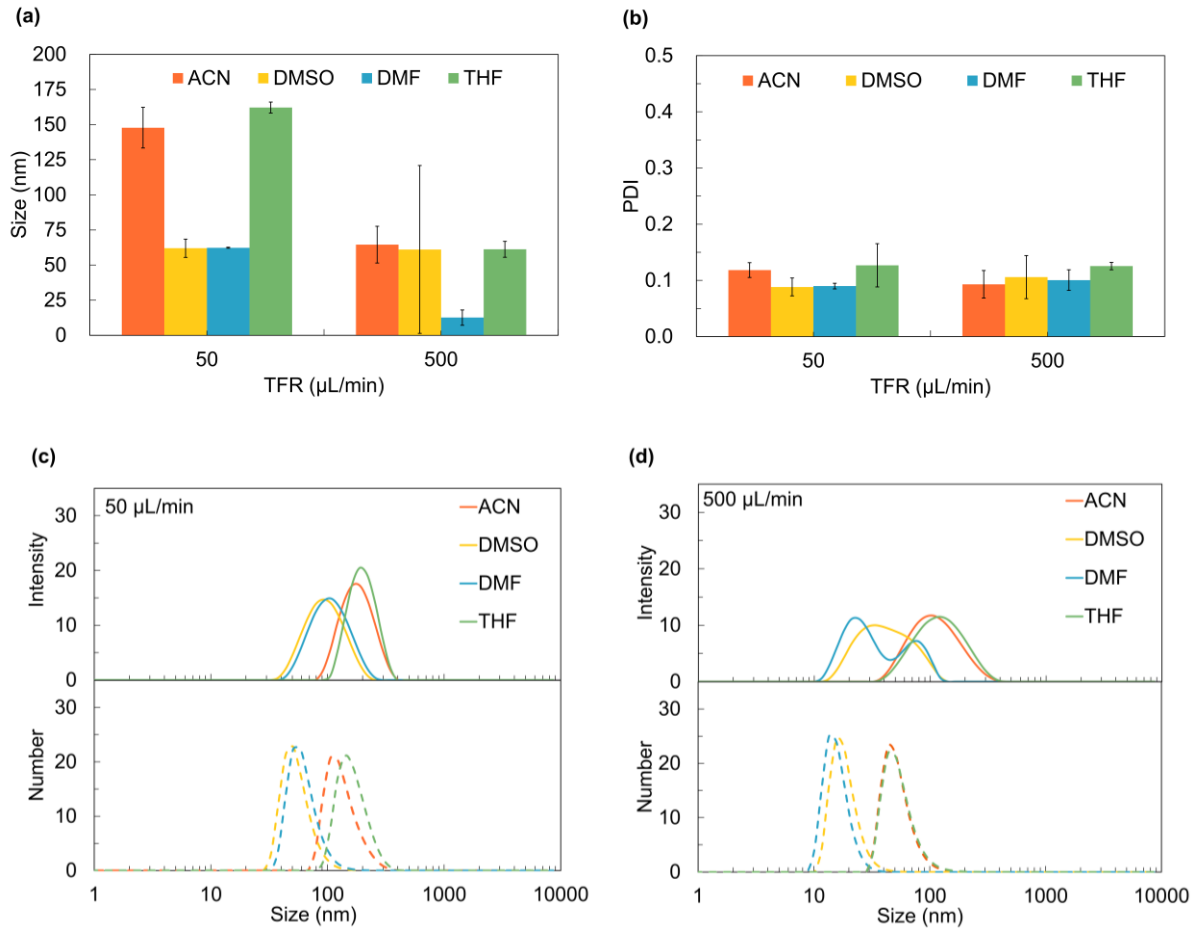

Fig 3.4 (a) Effect of the solvent properties on intensity-weighted and number-weighted NP size when the TFF is 50 or 500 µL/min; (b) PDI of prepared NPs; (c-d) NP size distribution prepared by four kinds of solvents: ACN, DMSO, DMF, and THF. Solid Lines represent the size distribution of intensity, while the dotted lines are numbers. The error bar represents the standard deviations from repeated experiments (at least three times). ACN (acetonitrile), DMSO (dimethyl sulfoxide), DMF (dimethylformamide), THF (tetrahydrofuran).

At low TFR, the NP sizes were 148 and 162 nm, respectively, when ACN and THF were

used as solvents. In contrast, when DMSO and DMF were used, the NP sizes were almost 60 nm. As shown in Table 3.1, THF showed the lowest viscosity, surface tension, polarity, and Hildebrand solubility, and the solvent properties of ACN were similar to these. In comparison with THF and ACN, DMF and DMSO showed higher viscosity, surface tension, polarity, and Hildebrand solubility parameters. This result agrees with previous reports where PLGA NPs were prepared by nanoprecipitation[31,39,42].

In addition, at a high TFR, the low repeatability or wide size distribution was attributed to the high viscosity and high surface tension of DMSO and DMF. As explained by the principle of the two-block polymer NPs' mechanism in microfluidic devices, the solvent exchange time (mixing time) of the organic solvent with water is essential[39]. Based on the Marangoni effect, the smaller surface tension difference between organic solvents and water means that mixing will be slower[43]. The surface tension difference between DMSO (or DMF) to water is small (Table 3.1), resulting in the broad particle size distribution of the particles prepared by DMSO and DMF (Fig 3.4(d)). Furthermore, Ostwald ripening is a phenomenon in which small particles are consumed by large particles during growth[44,45]. The viscosity of DMSO is very high, which further leads to a slowing down of solvent mixing, and further affects Ostwald ripening. Therefore, in the case of obtained particles with a wide particle size distribution, the higher viscosity leads to a different degree of ripening effect between batches, which in turn causes a lower reproducibility.

Based on these results, the screening range for size-modulated NPs preparation conditions may be enlarged, especially for a broader range of solvents. This will be resulting in a rapid and broad range of DDS screening and a significant step forward in later clinical settings.

3.3.3 Encapsulation of different kinds of anti-cancer drugs

Three different taxanes (PTX, CTX, and DTX) were used as model drugs. PTX and DTX are semisynthetic derivatives of 10-deacetylbaccatin-III. The natural PTX precursor molecule can be extracted from the European yew tree easily and sustainably. CTX, a novel second-generation taxane, is a dimethyl derivative of DTX bearing methoxy groups in place of the hydroxyl groups at the C-7 and C-10 positions.

ACN or THF was used as the solvent to prepare NPs with a concentration of 5 mg/mL of polymer, and the concentration of the drug being encapsulated was 0.5 mg/mL (10% of polymer). Similar to PTX-encapsulated NPs, CTX- and DTX-encapsulated NPs also decreased in size with increasing TFR, and no effect of solvent type on NP size was observed (Fig 3.5(a)). The encapsulation efficacies (EE) of the three different drugs in the NPs are shown in Fig 3.5(b). The EE of PTX was higher than those of CTX and DTX, regardless of TFR conditions. This can be attributed to PTX having the highest molecular weight. For the same mass concentration, a higher molecular weight means a lower amount of substance, and thus, less unencapsulation in the polymeric NPs; this implies a higher EE. In addition, the higher hydrophobicity of PTX is one of the reasons for its higher EE.

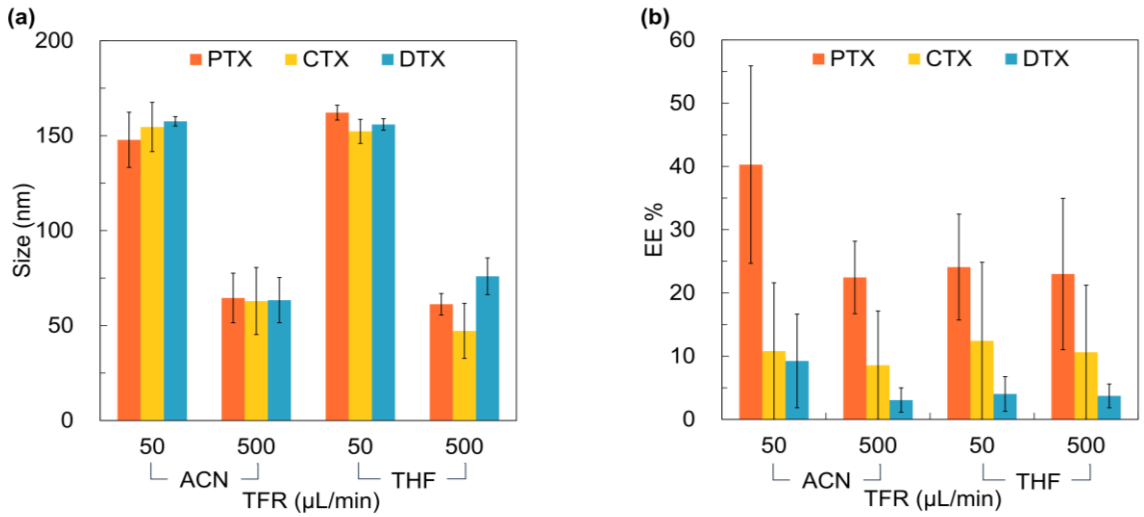

Fig 3.5 Difference of TFR or solvent on different kinds of drug-encapsulated NPs. (a) NPs size of PLGA-based NPs encapsulate PTX/CTX/DTX by employing ACN or THF as the solvent; (b) EE of drug-loaded NPs. The standard deviations were calculated from

3.3.4 Effect of PLGA NP size on cytotoxicity

Particles with different NP sizes were prepared to confirm that size-modulated NPs are useful for screening future DDS for clinical use. We used THF as the solvent; however, THF is not appropriate for the PDMS device. The NP size was modulated by varying only the TFR (50 or 500 μL/min) and encapsulating different types of taxane (PTX, CTX, DTX) anticancer drugs. These three drugs have similar mechanisms of action: binding to microtubule proteins and impairing the natural dynamics of microtubules, leading to mitotic arrest and apoptosis[46–48].

As shown in Fig 3.6, NPs encapsulated with the three different types of anticancer drugs showed NP size-dependent cell growth inhibition in HeLa cells after 24 h of incubation at drug concentrations ranging from 0.02 to 20 μg/mL. In HeLa cells incubated with PTX-loaded NPs,

the cell viability of those incubated with 62 nm NPs decreased from approximately 70% to approximately 36% with increasing PTX concentration, while that of cells incubated with 163 nm NPs decreased from 82% to 45%. The results for CTX-loaded NPs were similar to those for PTX; with increasing CTX concentrations, the cell viability decreased from 58% to 32% with 34 nm NPs and from 68% to 55% with 148 nm NPs. For DTX-NPs, the viability of HeLa cells incubated with 85 nm NPs decreased from 21% to 5%, while that with 154 nm NPs decreased from 47% to 38%. Overall, smaller NPs showed greater cytotoxicity. It has been previously shown that PLGA has a particle size effect on cellular uptake[19],[49],[50]. In addition, the toxicity to cells of particles of different particle sizes obtained by preparing ACN as a solvent was also studied (Fig 3.7). However, few studies focusing on in vitro NPs size effect using the NPs prepared by same polymer precursors. Our study fills this knowledge gap. Furthermore, our study demonstrated the ability of the glass-based microfluidic device to broaden the range of NPs preparation conditions, especially solvent conditions, compared to those using PDMS devices. These results strongly demonstrate the great potential of the glass-based microfluidic device as a large-scale screening device for the preparation of NPs for DDS and the establishment of a particle-size-controllable DDS

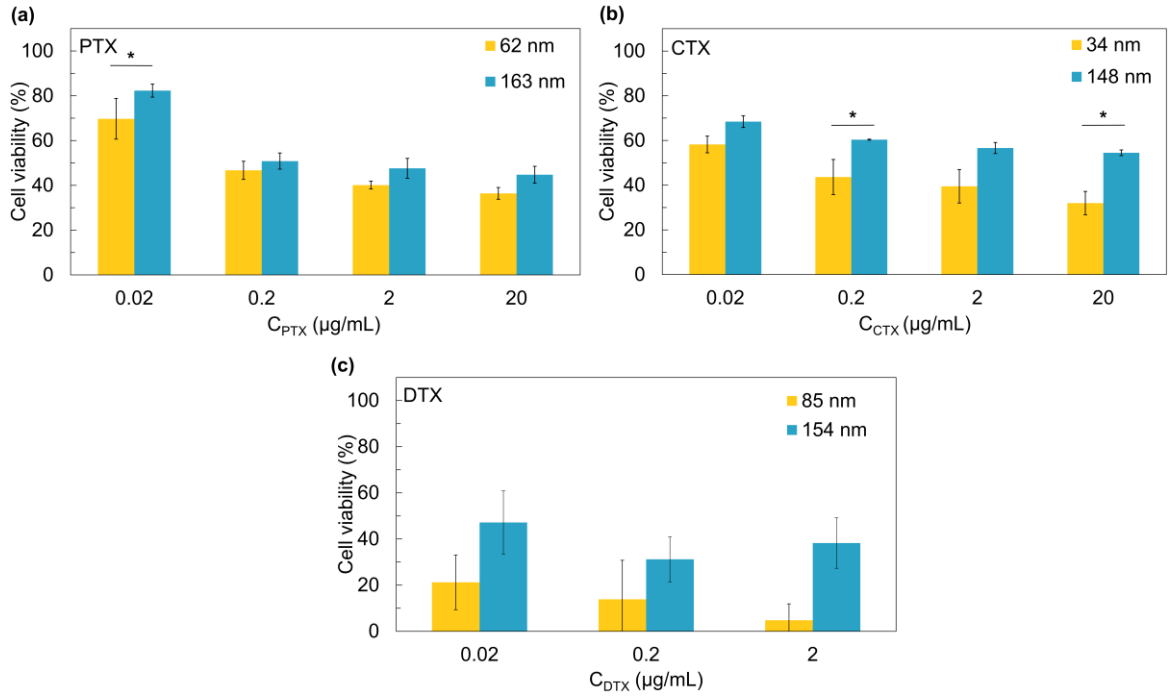

Fig 3.6 NP size effect on HeLa cell viability by incubated 24 h. NPs prepared by using THF as solvent. (a) PTX-loaded NPs; (b) CTX-loaded NPs; (c) DTX-loaded NPs. Standard deviations were calculated from the repeated experiment more than three times. P-values: *≤0.05.

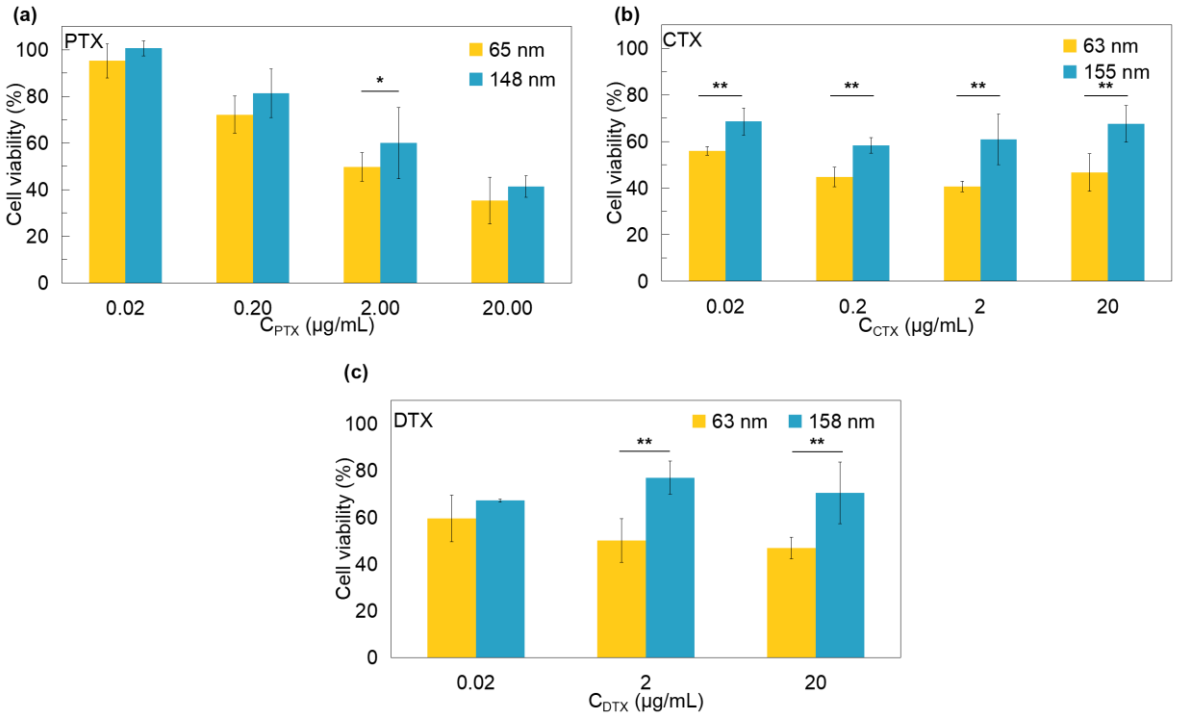

Fig 3.7 NP size effect on HeLa cell viability by incubated 24 h. NPs prepared by employing ACN as solvent. (a) PTX-loaded NPs; (b) CTX-loaded NPs; (c) DTX-loaded NPs. Standard deviations were calculated from the repeated experiment more than three times. P-values: *≤0.05.

3.4 Conclusions

In this study, we have explored the effect of condition, mainly for different organic solvents, for preparing size-modulated sub-200 nm PLGA NPs using a glass microfluidic device, without changing the polymer precursors. We also demonstrated the NP production of taxane-based anticancer drugs as model polymers and model pharmaceuticals. More specifically, under the preparative conditions of this study, ACN and THF were more suitable for preparing size-modulated NPs with narrower particle size distributions. In addition, PTX had a higher EE than CTX and DTX. Our results also showed the particle size impact of NPs on HeLa cells, regardless of the type of drug used in the in vitro studies. We believe that the

glass-based microfluidic device will serve as a powerful tool for effectively advancing drug screening and enbling tailored therapeutics in the future.

References

1. Sanjay ST, Zhou W, Dou M, Tavakoli H, Ma L, Xu F, et al. Recent advances of controlled drug delivery using microfluidic platforms. Advanced Drug Delivery Reviews. 2018;128: 3–28. doi:10.1016/J.ADDR.2017.09.013
2. Sanjay ST, Maowei D, Guanglei F, Feng X, Xiujun L. Controlled Drug Delivery Using Microdevices: Ingenta Connect. Current pharmaceutical biotechnology. 2016;17: 772–787. Available: https://www.ingentaconnect.com/content/ben/cpb/2016/00000017/00000009/art00004
3. Thomas OS, Weber W. Overcoming Physiological Barriers to Nanoparticle Delivery—Are We There Yet? Frontiers in Bioengineering and Biotechnology. 2019; 415. doi:10.3389/FBIOE.2019.00415/BIBTEX
4. Moura RP, Martins C, Pinto S, Sousa F, Sarmento B. Blood-brain barrier receptors and transporters: an insight on their function and how to exploit them through nanotechnology. Expert opinion on drug delivery. 2019;16: 271–285. doi:10.1080/17425247.2019.1583205
5. Sur S, Rathore A, Dave V, Reddy KR, Chouhan RS, Sadhu V. Recent developments in functionalized polymer nanoparticles for efficient drug delivery system. Nano-Structures & Nano-Objects. 2019;20: 100397. doi:10.1016/J.NANOSO.2019.100397
6. Wilczewska AZ, Niemirowicz K, Markiewicz KH. Nanoparticles as drug delivery systems. Pharmacological reports. 2012;64: 1020–1037. doi:10.1016/S1734-1140(12)70901-5
7. Riehemann K, Schneider SW, Luger TA, Godin B, Ferrari M, Fuchs H. Nanomedicine - Challenge and perspectives. Angewandte Chemie - International Edition. 2009;48: 872–897. doi:10.1002/anie.200802585
8. Lepeltier E, Bourgaux C, Couvreur P. Nanoprecipitation and the “Ouzo effect”: Application to drug delivery devices. Advanced Drug Delivery Reviews. Elsevier; 2014. pp. 86–97. doi:10.1016/j.addr.2013.12.009
9. McNeil SE. Nanotechnology for the biologist. Journal of Leukocyte Biology. 2005;78: 585–594. doi:10.1189/jlb.0205074
10. Danhier F, Ansorena E, Silva JM, Coco R, Le Breton A, Préat V. PLGA-based nanoparticles: An overview of biomedical applications. Journal of Controlled Release. 2012;161: 505–522. doi:10.1016/J.JCONREL.2012.01.043

11. Kumari A, Yadav SK, Yadav SC. Biodegradable polymeric nanoparticles based drug delivery systems. Colloids and Surfaces B: Biointerfaces. 2010. pp. 1–18. doi:10.1016/j.colsurfb.2009.09.001
12. Pandita D, Kumar S, Lather V. Hybrid poly(lactic-co-glycolic acid) nanoparticles: design and delivery prospectives. Drug Discovery Today. 2015;20: 95–104. doi:10.1016/J.DRUDIS.2014.09.018
13. Zhang Z, Wang X, Li B, Hou Y, Yang J, Yi L. Development of a novel morphological paclitaxel-loaded PLGA microspheres for effective cancer therapy: In vitro and in vivo evaluations. Drug Delivery. 2018;25: 166–177. doi:10.1080/10717544.2017.1422296
14. Acharya S, Sahoo SK. PLGA nanoparticles containing various anticancer agents and tumour delivery by EPR effect. Advanced Drug Delivery Reviews. 2011;63: 170–183. doi:10.1016/J.ADDR.2010.10.008
15. Cheng J, Teply BA, Sherifi I, Sung J, Luther G, Gu FX, et al. Formulation of functionalized PLGA-PEG nanoparticles for in vivo targeted drug delivery. Biomaterials. 2007;28: 869–876. doi:10.1016/j.biomaterials.2006.09.047
16. Bhardwaj V, Ankola DD, Gupta SC, Schneider M, Lehr CM, Kumar MNVR. PLGA nanoparticles stabilized with cationic surfactant: Safety studies and application in oral delivery of paclitaxel to treat chemical-induced breast cancer in rat. Pharmaceutical Research. 2009;26: 2495–2503. doi:10.1007/S11095-009-9965-4/FIGURES/8
17. Zhou W, Dou M, Timilsina SS, Xu F, Li XJ. Recent innovations in cost-effective polymer and paper hybrid microfluidic devices. Lab on a Chip. 2021;21: 2658–2683. doi:10.1039/D1LC00414J
18. Chiu HI, Samad NA, Fang L, Lim V. Cytotoxicity of targeted PLGA nanoparticles: a systematic review. RSC Advances. Royal Society of Chemistry; 2021. pp. 9433–9449. doi:10.1039/d1ra00074h
19. Choi JS, Cao J, Naeem M, Noh J, Hasan N, Choi HK, et al. Size-controlled biodegradable nanoparticles: Preparation and size-dependent cellular uptake and tumor cell growth inhibition. Colloids and Surfaces B: Biointerfaces. 2014;122: 545–551. doi:10.1016/J.COLSURFB.2014.07.030
20. Breunig M, Bauer S, Goepferich A. Polymers and nanoparticles: Intelligent tools for intracellular targeting? European Journal of Pharmaceutics and Biopharmaceutics. Elsevier; 2008. pp. 112–128. doi:10.1016/j.ejpb.2007.06.010
21. Madani F, Esnaashari SS, Mujokoro B, Dorkoosh F, Khosravani M, Adabi M. Investigation of effective parameters on size of paclitaxel loaded PLGA nanoparticles.

Advanced Pharmaceutical Bulletin. 2018;8: 77–84. doi:10.15171/apb.2018.010

22. Shah N, Chaudhari K, Dantuluri P, Murthy RSR, Das S. Paclitaxel-loaded PLGA nanoparticles surface modified with transferrin and Pluronic®P85, an in vitro cell line and in vivo biodistribution studies on rat model. Journal of Drug Targeting. 2009;17: 533–542. doi:10.1080/10611860903046628
23. Rhee M, Valencia PM, Rodriguez MI, Langer R, Farokhzad OC, Karnik R. Synthesis of Size-Tunable Polymeric Nanoparticles Enabled by 3D Hydrodynamic Flow Focusing in Single-Layer Microchannels. Advanced Materials. 2011;23: H79–H83. doi:10.1002/adma.201004333
24. Valencia PM, Basto PA, Zhang L, Rhee M, Langer R, Farokhzad OC, et al. Single-Step Assembly of Homogenous Lipid−Polymeric and Lipid−Quantum Dot Nanoparticles Enabled by Microfluidic Rapid Mixing. ACS Nano. 2010;4: 1671–1679. doi:10.1021/nn901433u
25. Damiati S, Kompella UB, Damiati SA, Kodzius R. Microfluidic devices for drug delivery systems and drug screening. Genes. MDPI AG; 2018. p. 103. doi:10.3390/genes9020103
26. Maeki M, Okada Y, Uno S, Niwa A, Ishida A, Tani H, et al. Production of siRNA-Loaded Lipid Nanoparticles using a Microfluidic Device. Journal of visualized experiments. 2022; e62999. doi:10.3791/62999
27. Maeki M, Uno S, Niwa A, Okada Y, Tokeshi M. Microfluidic technologies and devices for lipid nanoparticle-based RNA delivery. Journal of Controlled Release. 2022;344: 80–96. doi:10.1016/J.JCONREL.2022.02.017
28. Kimura N, Maeki M, Sasaki K, Sato Y, Ishida A, Tani H, et al. Three-dimensional, symmetrically assembled microfluidic device for lipid nanoparticle production. RSC Advances. 2021;11: 1430–1439. doi:10.1039/D0RA08826A
29. Dou M, García JM, Zhan S, Li XJ. Interfacial nano-biosensing in microfluidic droplets for high-sensitivity detection of low-solubility molecules. Chemical Communications. 2016;52: 3470–3473. doi:10.1039/C5CC09066K
30. Lv M, Zhou W, Tavakoli H, Bautista C, Xia J, Wang Z, et al. Aptamer-functionalized metal-organic frameworks (MOFs) for biosensing. Biosensors and Bioelectronics. 2021;176: 112947. doi:10.1016/J.BIOS.2020.112947
31. López RR, G. Font de Rubinat P, Sánchez LM, Tsering T, Alazzam A, Bergeron KF, et al. The effect of different organic solvents in liposome properties produced in a periodic disturbance mixer: Transcutol®, a potential organic solvent replacement. Colloids and

Surfaces B: Biointerfaces. 2021;198: 111447. doi:10.1016/J.COLSURFB.2020.111447

32. Wischke C, Schwendeman SP. Principles of encapsulating hydrophobic drugs in PLA/PLGA microparticles. International Journal of Pharmaceutics. 2008;364: 298–327. doi:10.1016/J.IJPHARM.2008.04.042
33. Lepeltier E, Bourgaux C, Couvreur P. Nanoprecipitation and the “Ouzo effect”: Application to drug delivery devices. Advanced Drug Delivery Reviews. 2014;71: 86–97. doi:10.1016/J.ADDR.2013.12.009
34. Allen C, Maysinger D, Eisenberg A. Nano-engineering block copolymer aggregates for drug delivery. Colloids and Surfaces B: Biointerfaces. 1999;16: 3–27. doi:10.1016/S0927-7765(99)00058-2
35. Lee JN, Park C, Whitesides GM. Solvent Compatibility of Poly(dimethylsiloxane)-Based Microfluidic Devices. Analytical Chemistry. 2003;75: 6544–6554. doi:10.1021/AC0346712
36. Toepke MW, Beebe DJ. PDMS absorption of small molecules and consequences in microfluidic applications. Lab on a Chip. 2006;6: 1484–1486. doi:10.1039/B612140C
37. Ren K, Zhou J, Wu H. Materials for microfluidic chip fabrication. Accounts of Chemical Research. 2013;46: 2396–2406. doi: 10.1021/ar300314s
38. Tang T, Yuan Y, Yalikun Y, Hosokawa Y, Li M, Tanaka Y. Glass based micro total analysis systems: Materials, fabrication methods, and applications. Sensors and Actuators B: Chemical. 2021;339: 129859. doi:10.1016/J.SNB.2021.129859
39. Karnik R, Gu F, Basto P, Cannizzaro C, Dean L, Kyei-Manu W, et al. Microfluidic Platform for Controlled Synthesis of Polymeric Nanoparticles. Nano Letters. 2008;8: 2906–2912. doi:10.1021/nl801736q
40. Legrand P, Lesieur S, Bochot A, Gref R, Raatjes W, Barratt G, et al. Influence of polymer behaviour in organic solution on the production of polylactide nanoparticles by nanoprecipitation. International Journal of Pharmaceutics. 2007;344: 33–43. doi:10.1016/J.IJPHARM.2007.05.054
41. Perrie Y, Webb C, Khadke S, Schmidt ST, Roces CB, Forbes N, et al. The Impact of Solvent Selection: Strategies to Guide the Manufacturing of Liposomes Using Microfluidics. Pharmaceutics 2019, Vol 11, Page 653. 2019;11: 653. doi:10.3390/PHARMACEUTICS11120653
42. Shepherd SJ, Issadore D, Mitchell MJ. Microfluidic formulation of nanoparticles for biomedical applications. Biomaterials. 2021;274: 120826. doi:10.1016/J.BIOMATERIALS.2021.120826

43. Sternling C V., Scriven LE. Interfacial turbulence: Hydrodynamic instability and the marangoni effect. AIChE Journal. 1959;5: 514–523. doi:10.1002/AIC.690050421
44. Wagner C, Wagner C. Theorie der Alterung von Niederschlägen durch Umlösen (Ostwald-Reifung). Zeitschrift für Elektrochemie, Berichte der Bunsengesellschaft für physikalische Chemie. 1961;65: 581–591. doi:10.1002/BBPC.19610650704
45. Lifshitz IM, Slyozov V V. The kinetics of precipitation from supersaturated solid solutions. Journal of Physics and Chemistry of Solids. 1961;19: 35–50. doi:10.1016/0022-3697(61)90054-3
46. Jordan MA, Wilson L. Microtubules as a target for anticancer drugs. Nature Reviews Cancer. 2004;4: 253–265. doi:10.1038/nrc1317
47. Paller CJ, Antonarakis ES. Cabazitaxel: a novel second-line treatment for metastatic castration-resistant prostate cancer. Drug Design, Development and Therapy. 2011;5: 117. doi:10.2147/DDDT.S13029
48. Calcagno F, Nguyen T, Dobi E, Villanueva C, Curtit E, Kim S, et al. Safety and efficacy of cabazitaxel in the docetaxel-treated patients with hormone-refractory prostate cancer. Clinical Medicine Insights Oncology. 2013;7: 1–12. doi:10.4137/CMO.S7256
49. Xu A, Yao M, Xu G, Ying J, Ma W, Li B, et al. A physical model for the size-dependent cellular uptake of nanoparticles modified with cationic surfactants. International Journal of Nanomedicine. 2012;7: 3547–3554. doi:10.2147/IJN.S32188
50. Busatto C, Pesoa J, Helbling I, Luna J, Estenoz D. Effect of particle size, polydispersity and polymer degradation on progesterone release from PLGA microparticles: Experimental and mathematical modeling. International Journal of Pharmaceutics. 2018;536: 360–369. doi:10.1016/j.ijpharm.2017.12.006

CHAPTER 4 Conclusion and future prospects

4.1 Conclusion

This study focuses on more refinement and broadening the selectivity of custom designed PLGA nanoparticles (NPs). In terms of refinement, it is important to accomplish the preparation of various particle sizes without changing the polymer precursors. In terms of broadening the selectivity, the most important thing is to broaden the effective selectivity size of nanoparticles prepared below 200 nm for the drug delivery system (DDS). Secondly, it also broadens the choice of organic solvents. The wide choice of organic solvents means that the universality of different solubility drugs for drug screening can be expanded, thus providing researchers with a wider range of choices. This method of preparation is simple, efficient, low labor, and low cost, which are important factors to consider in order to achieve rapid drug screening to obtain "optimal solutions" for NPs for different diseases or conditions. The following is a general overview of the current research.

In Chapter 2, the iLiNP™ device was used for the preparation of polymeric NPs. The particles obtained were well prepared to exhibit a large selectable range of particle sizes (PLGA NPs: 44-101 nm; PEG-PLGA NPs: 29-76 nm; blend NPs: 40-114 nm), while the conventional nanoprecipitation method can only yield a narrow selectable range of particle sizes (PLGA NPs: 80-87 nm; PEG-PLGA NPs: 64-68 nm; blend NPs: 81-90 nm). Moreover, this good preparation performance was maintained not only in the blank particles but also after the NPs were encapsulated with the anticancer drug paclitaxel (PTX). The encapsulated PTX-loaded NPs showed different growth inhibition of breast cancer cells HeLa cells with respect to particle size. This confirms the biotherapeutic significance of providing a variety of rich particle size options

under the same polymer precursor preparation conditions.

In chapter 3, I further broaden and improve the solvent restriction of the PDMS iLiNP device. I try to explore the solvent screening for NPs preparation that can be achieved with high solvent selectivity using a glass-prepared device, which is unsuitable for many organic solvents since it faces swelling when exposed to many organic solvents, point of separation from the glass substrate. However, different drugs have different solubilities for different organic solvents, which implies the need to provide drug screening and optimization of solvent conditions that can be performed with different solvents. In this section, we have tried to perform solvent screening using four solvents: acetonitrile (ACN), dimethyl sulfoxide (DMSO), dimethylformamide (DMS), and tetrahydrofuran (THF). The results show that the use of ACN and THF is more suitable for particle size control in the device. In addition, three different paclitaxel drugs, paclitaxel (PTX), cabazitaxel (CTX), and docetaxel (DTX), were encapsulated, with PTX showing a higher encapsulation rate. NPs of different particle sizes in HeLa cells showed particle size-dependent cell toxicity. Thus, the glass device further broadens the solvent-screenable range of PLGA-based NPs with a large range of customized particle sizes, which implies breaking the condition-bound of more particle customization and provides a powerful method for drug screening.

4.2 Implications of the research and relationship to previous research

This section will discuss the Implications of the present study in this research area, and their relationship with previous studies. In this study, customized PLGA-based NPs were

prepared using the iLiNP device, with more emphasis on "refinement" and "rich selectivity". The PLGA NPs were prepared with a wide particle size selectivity of sub-200 nm, and could also withstand screening with different solvent conditions and different drugs. The encapsulation rate is also better, and in addition, the results of in vitro studies show that particle size tailoring is of importance. This method can provide the future need for particle size tailoring with a wide range of selective conditions and high precision (same polymer, different particle sizes) and has the potential to be utilized in a variety of different fields.

Chapter 2 is explored the preparation of NPs with a large range of particle size selectivity. Most previous microfluidic device studies have varied polymer precursors (including the molecular weight of the polymer, the concentration of the solution, the chain composition of the polymer, etc.) in order to achieve a wider range of particle size selectivity in the prepared particles[1–3]. First, let us discuss the implications of not changing the precursor: 1) In terms of labor consumption, changing the polymer precursor means a different formulation of the solution injected into the microfluidic device, which requires more labor-intensive operations. However, this would undermine the powerful advantages of the microfluidic device - a non-labor-intensive approach. 2) In addition, a more important aspect is the customization of the particles. If the polymer precursor is changed to change the particle size, the difference in the particles would not only be the particle size, but also the effect of the inherent precursor properties on the particles. The particles obtained by such customization will not be sufficiently refined for "particle size" only. Because of this limitation, many studies on the effect of particle size, where the difference between particles is not only the particle size but also the precursors of the polymer, cannot be precisely attributed to the effect of particle size on the final result.

Secondly, I will start with the important point about more selectivity: due to the narrow selectivity of the same method for particle size, when studying the effect of particle size, etc., the researcher is through different preparation methods to achieve the different particle size preparation[4]. That also implies a question, is the effect of the final obtained particle size different on the experimental results only attributed to the particle size? Or does the preparation method also have a non-negligible effect?

All of these limits further refinement of the effect of particle size on NPs from biodistribution, to biochemical properties, and so on. To a greater extent of utilization, it is not possible to tailor the properties ideally enough for future customized treatments. And this research can fill this gap, offering the possibility of specific polymer particle size customization and diversified particle size selection.

In Chapter 3, a glass iLiNP device is provided to prepare NPs and screen the solvent. Previous studies on the formation of polymer particles by solvents have been well explored[5–8]. However, in microfluidic devices, solvent screening has only been explored in a simple capillary design, without any lattice design in the flow path[9]. From the study in Chapter 2, it is clear that iLiNP devices can provide a wider range of particle size selectivity. Then, the broadening of the solvent breadth in the iLiNP device for the preparation of PLGA-based NPs with solvent exploration is still very necessary. . This study achieves the advancement of diversified solvent selection based on the preparation of customized particle size for the preparation of immobilized polymer precursors, and furthermore expands the screening range for various conditions.

4.3 Limitation of this research and future prospect

The limitations and proposed recommendations regarding this study will be stated as follows.

First, both PDMS devices and glass devices still cannot solve the problem that hydrophobic polymers are highly prone to accumulate on the inner wall of the channel and eventually lead to clogging of the device. This requires the exploration of appropriate wall modification methods that will not be stripped by the organic solvents commonly used for preparation. Alternatively, it is necessary to explore the possibility of forming a liquid sheath with an insoluble liquid on the outside of this complex fluidic process to prevent the contact of the polymer solution with the inner wall of the microfluidic device, thus preventing clogging.

In addition, in Chapter 3, the effect of solvent type on the size and particle size distribution of the formed particles is explored. However, in flow focus microfluidic devices, a large part of the low encapsulation rate of the drug is due to the difference in the precipitation time scale of the drug and the precipitation time scale of the polymer. Since the glass device already promises a high tolerance of different organic solvents. Then a good use of the solvent advantage to finalize the formulation of different solvents and thus adjust the drug to polymer with a more similar settling time is highly desirable to greatly improve the drug encapsulation rate.

Third, the device design used is optimal for iLiNP when dissolved in ethanol, but does this optimal solution design still remain optimal for polymers dissolved in different organic solvents as well? The design of different channels still needs to be explored. The device design can be optimized by performing fluid simulations using COSMOL software and corroborated by actual experimental operations.

Fourth, although this device promises a simple, and time-saving way to prepare PLGA, however, if the mixing of many different solvent formulations is required and still requires manual replacement of the syringe. In the modern era where information technology is highly developed and widely utilized, the addition of multiple inlet channels to this device can be considered and programmed to control the injection of syringes containing different solvents can be programmed to be injected separately. This would greatly liberate productivity.

References

1. Valencia PM, Basto PA, Zhang L, Rhee M, Langer R, Farokhzad OC, et al. Single-Step Assembly of Homogenous Lipid−Polymeric and Lipid−Quantum Dot Nanoparticles Enabled by Microfluidic Rapid Mixing. ACS Nano. 2010;4: 1671–1679. doi:10.1021/nn901433u
2. Valencia PM, Pridgen EM, Rhee M, Langer R, Farokhzad OC, Karnik R. Microfluidic Platform for Combinatorial Synthesis and Optimization of Targeted Nanoparticles for Cancer Therapy. ACS Nano. 2013;7: 10671–10680. doi:10.1021/nn403370e
3. Karnik R, Gu F, Basto P, Cannizzaro C, Dean L, Kyei-Manu W, et al. Microfluidic Platform for Controlled Synthesis of Polymeric Nanoparticles. Nano Letters. 2008;8: 2906–2912. doi:10.1021/nl801736q
4. Choi JS, Cao J, Naeem M, Noh J, Hasan N, Choi HK, et al. Size-controlled biodegradable nanoparticles: Preparation and size-dependent cellular uptake and tumor cell growth inhibition. Colloids and Surfaces B: Biointerfaces. 2014;122: 545–551. doi:10.1016/J.COLSURFB.2014.07.030
5. Jeon HJ, Jeong Y Il, Jang MK, Park YH, Nah JW. Effect of solvent on the preparation of surfactant-free poly(dl-lactide-co-glycolide) nanoparticles and norfloxacin release characteristics. International Journal of Pharmaceutics. 2000;207: 99–108. doi:10.1016/S0378-5173(00)00537-8
6. Song KC, Lee HS, Choung IY, Cho KI, Ahn Y, Choi EJ. The effect of type of organic phase solvents on the particle size of poly(d,l-lactide-co-glycolide) nanoparticles. Colloids and Surfaces A: Physicochemical and Engineering Aspects. 2006;276: 162–167. doi:10.1016/J.COLSURFA.2005.10.064
7. Sahana DK, Mittal G, Bhardwaj V, Kumar MNVR. PLGA Nanoparticles for Oral Delivery of Hydrophobic Drugs: Influence of Organic Solvent on Nanoparticle Formation and Release Behavior In Vitro and In Vivo Using Estradiol as a Model Drug. Journal of Pharmaceutical Sciences. 2008;97: 1530–1542. doi:10.1002/JPS.21158
8. Almoustafa HA, Alshawsh MA, Chik Z. Technical aspects of preparing PEG-PLGA nanoparticles as carrier for chemotherapeutic agents by nanoprecipitation method.

International Journal of Pharmaceutics. 2017;533: 275–284. doi:10.1016/J.IJPHARM.2017.09.054

9. Lababidi N, Sigal V, Koenneke A, Schwarzkopf K, Manz A, Schneider M. Microfluidics as tool to prepare size-tunable PLGA nanoparticles with high curcumin encapsulation for efficient mucus penetration. Beilstein Journal of Nanotechnology. 2019;10: 2280–2293. doi:10.3762/bjnano.10.220

Acknowledgment

After five years of study at Hokkaido University, this thesis was finally accomplished. While completing my studies, I also experienced the COVID-19 pandemic in the whole world, these special experiences will be a precious memory which I will never forget. Here I would like to express my sincere gratitude for peoples who have given me great amount of help, without them I could not complete my studies.

First of all, I would like to thank from the bottom of my heart to my cordial supervisor, Professor Tokeshi. I am very grateful to him for giving me the valuable opportunity to experience studying in Japan. Five years ago, my life took a huge turn because of an email from him. He is always very kind and responsive to my requests for help not only in research but also in all aspects of life. Secondly, I would like to thank Maeki-sensei, who has helped me a lot in my experiments and research. I have learned a lot from his rigorous approach to science, and I have improved my ability to handle my research and resolve my mental state under high pressure. I am also grateful to Tani-sensei, and Ishida-sensei for their kindly help in the lab.

Next, I would like to thank my friends who have been there for me during these bittersweet days. Thanks to my friends who are always willing to help me digest my negative emotions, listen to me on countless nights when I had a breakdown, and lend me a helping hand. With their help, I gradually came to terms with everything about myself and emerged from my depression. Thank you to my Chinese friends and the international friends I met at the lab. I wish you all a bright future and a toast to our friendship.

Finally, I would like to give my deep gratitude to my parents. I would never have

accomplished what I have accomplished without their dedication over the years. They have supported me in my study abroad life even though they were not in a particularly good financial situation. I hope I can also become an excellent woman as gentle and strong as my mother.